Biogeosciences Discuss., 6, 4639–4692, 2009
www.biogeosciences-discuss.net/6/4639/2009/

Biogeosciences Discussions

Biogeosciences Discussions is the access reviewed discussion forum of *Biogeosciences*

Variations in leaf physiological properties within Amazon forest canopies

J. Lloyd[1], S. Patiño[2], R. Q. Paiva[3,*], G. B. Nardoto[4], C. A. Quesada[1,3,5], A. J. B. Santos[3,5,†], T. R. Baker[1], W. A. Brand[6], I. Hilke[6], H. Gielmann[6], M. Raessler[6], F. J. Luizão[3], L. A. Martinelli[4], and L. M. Mercado[7]

[1]Earth and Biosphere Institute, School of Geography, University of Leeds, LS2 9JT, UK
[2]Grupo de Ecología de Ecosistemas Terrestres Tropicales, Universidad Nacional de Colombia, Sede Amazonia, Instituto Amazónico de Investigaciones-Imani, km. 2, vía Tarapacá, Leticia, Amazonas, Colombia
[3]Institito National de Pesquisas Amazônicas, Manaus, Brazil
[4]Centro de Energia Nuclear na Agricultura, Av. Centenário 303, 13416-000, Piracicaba-SP, Brazil
[5]Departamento de Ecologia, Universidade de Brasília, DF, Brazil
[6]Max-Planck-Institut für Biogeochemie, Postfach 100164, 07701, Jena, Germany
[7]Centre for Ecology and Hydrology, Wallingford, UK

[*] now at: Secretária Municipal de Desenvolvimento e Meio Ammbiente ma Prefeturia Municipal de Maués, Maués, Brazil
[†] Alexandre Santos died in the Amazon plane crash of 29 September 2006

Received: 18 December 2008 – Accepted: 3 February 2009 – Published: 5 May 2009

Correspondence to: J. Lloyd (j.lloyd@leeds.ac.uk)

Published by Copernicus Publications on behalf of the European Geosciences Union.

Abstract

Vertical profiles in leaf mass per unit leaf area (M_A), foliar ^{13}C composition ($\delta^{13}C$) and leaf nitrogen (N), phosphorus (P), carbon (C), potassium (K), magnesium (Mg) and calcium (Ca) concentrations were estimated for 204 rain forest trees growing in 57 sites across the Amazon Basin. Data was analysed using a multilevel modelling approach, allowing a separation of gradients within individual tree canopies (intra-tree gradients) as opposed to stand level gradients occurring because of systematic differences occurring between different trees of different heights (inter-tree gradients). Significant positive intra-tree gradients (i.e. increasing values with increasing sampling height) were observed for M_A and $[C]_{DW}$ (the subscript denoting on a dry weight basis) with negative intra-tree gradients observed for $\delta^{13}C$, $[Mg]_{DW}$ and $[K]_{DW}$. No significant intra-tree gradients were observed for $[N]_{DW}$, $[P]_{DW}$ or $[Ca]_{DW}$. Although the magnitudes of inter-tree gradients were not significantly different for M_A, $\delta^{13}C$, $[C]_{DW}$, $[K]_{DW}$, $[N]_{DW}$, $[P]_{DW}$ and $[Ca]_{DW}$, for $[Mg]_{DW}$ there no systematic difference observed between trees of different heights, this being in contrast to the strongly negative intra-tree gradients also found to exist.

When expressed on a leaf area basis, significant positive gradients were observed for N, P and K both within and between trees, these being attributable to the positive intra- and inter-tree gradients in M_A mentioned above. No systematic intra-tree gradient was observed for either Ca or Mg when expressed on a leaf area basis, but with a significant positive gradient observed for Mg between trees (i.e. with taller trees tending to have a higher Mg per unit area).

In contrast to the other variables measured, significant variations in intra-tree gradients for different individuals were found to exist for M_A, $\delta^{13}C$ and [P] (area basis). This was best associated with the overall average area based [P], this also being considered to be a surrogate for a leaf's photosynthetic capacity, A_{max}. A new model is presented which is in agreement with the above observations. The model predicts that trees characterised by a low upper canopy A_{max} should have shallow or even non-

BGD

6, 4639–4692, 2009

existent gradients in A_{max}, with optimal intra-canopy gradients becoming sharper as a tree's upper canopy A_{max} increases. Nevertheless, in all cases it is predicted that the optimal within-canopy gradients in A_{max} should be less than is generally observed for photon irradiance. Although this is consistent with numerous observations, it is also in contrast to previously held notions of optimality.

1 Introduction

It has long been observed that the light saturated photosynthetic rates of leaves located low in plant canopies can be typically much less than leaves receiving much more irradiance (Q) higher up (Jarvis et al., 1976) and this has been typically attributed to gradients in foliar nitrogen contents on a leaf area basis (Field, 1983). Nitrogen is a critical component of the photosynthetic apparatus (Evans, 1989) and it been shown that a theoretically optimal distribution of nitrogen concentration maximizes canopy photosynthesis when nitrogen concentrations closely follows the distribution of Q, approaching zero when Q also does (Field, 1983; Chen et al., 1993). Nevertheless, one regular observation in tree canopies seems to be that vertical gradients in photosynthetic capacity seem to be much less than that which would be optimal to maximise individual plant carbon gain (e.g. Hollinger, 1996; Kull and Niinemets, 1998; Meir et al., 2002; Wright et al., 2006).

Understanding and quantifying within canopy gradients in photosynthetically important nutrient and associated changes in plant physiological properties is also important for simulating rates of canopy photosynthesis and the associated light response (Lloyd et al., 1995; Haxeltine and Prentice, 1996; de Pury and Farquhar, 1997) as well as for simulations of canopy leaf areas (themselves affecting predicted rates of photosynthetic carbon gain) in dynamic vegetation models (Sitch et al., 2003; Woodward and Loomis, 2004). Within tropical forest canopies, this variation may be expected to be especially complicated due to the very high number of species present in any one forest with an associated high tree-to-tree variation, at least some of which can be related

to asymptotic tree height (Lloyd et al., 1995; Thomas and Bazzaz, 1999; Rijkers et al., 2000) successional status (Popma et al., 1992; Reich et al., 1995) and/or shade tolerance (Turner, 2001). Mean vertical variations in nutrient concentrations and associated physiological characteristics within tropical forests may thus be as much due to tree-to-tree variations correlated with actual or potential tree height as with variations within individual trees themselves. Nitrogen need not, of course, always the primary limiting nutrient for photosynthesis in higher plants (Field and Mooney, 1986), especially for tropical forest trees who's photosynthetic rates are also closely correlated with foliar phosphorus content (Cromer et al., 1993; Raaimakers et al., 1995; Reich et al., 1995; Lovelock et al., 1997).

We here analyse vertical variations in leaf properties for 204 trees sampled at a range of locations across Amazonia, attempting to quantify variations in foliar nutrient concentrations, isotopic composition and M_A with height. As well as analysing this observational data, we also present a new model which shows that the true "optimal" gradient in plant canopies to not necessarily mimic the gradient in Q. This model, described immediately below, is predicated on the observation that foliar leaf nutrient concentrations are to a large degree genetically determined (Fyllas et al., 2009) and thus for any given species there is a practical limit to what value leaves at the top of the canopy can assume. Once this is taken into account, it emerges that trees with a low overall photosynthetic potential should have a shallow (or even zero) decline in photosynthetic capacity with canopy depth, with higher photosynthetic capacity trees having sharper gradients for the optimisation of canopy photosynthesis. Data from a range of Amazon forest trees presented here shows this to be the case.

2 Theoretical considerations

The model used to evaluate the optimal distribution of resources for species of a fixed maximum photosynthetic capacity is outlined in the Appendix. In short, it consists of the use integral equations combining gradients in photosynthetically active radiation,

Q, photosynthetic capacity, A and leaf respiration, R throughout plant canopies, also allowing for leaf respiration rates to be reduced at higher irradiances (Atkin et al., 2000).

2.1 Simulations with a canopy of fixed photosynthetic capacity

We first apply the model above to a rainforest canopy with a leaf area index, L, of either 2.0, 5.0 or 8.0 but in all cases having the same photosynthetic capacity C_C. To obtain a realistic estimate a of the latter, we took representative observational values from data presented by Domingues et al. (2005) for a forest near Tapajos viz. L=5.5, A_0^*=12.0 µmol m^{-2} s^{-1} (full sunlight) and with an extinction coefficient for photosynthetic capacity, k_P, of 0.15. Taking then a simple integral equation, we obtain

$$C_C = A_0^* e^{-k_P z}\Big|_{z=0}^{z=L} = \frac{A_0^*(1 - e^{-k_P L})}{k_P}, \quad (1)$$

where A_0^* is the CO_2 assimilation rate at the top of the canopy (ignoring dark respiration) we obtain C_C=42 µmol m^{-2} s^{-1} (ground area basis). Now, keeping this canopy photosynthetic potential constant, the first question we ask in a series of investigative simulations is how should the canopy photosynthetic rate, A_C^*, vary across a range of potential k_p? And how is this variation in A_C^* with k_P influenced by L? To do this we use Eq. (A4) and Eq. (A5) as detailed in the Appendix.

For these simulations, we always use a value for the light extinction with the canopy of k_l=0.7 as reported for tropical forest (Wirth et al., 2001). Because C_C is held constant for all simulations, this requires that A_0^* varies as k_P changes This is achieved *via* a rearrangement of Eq. (1) ; viz $A_0^*=k_P C_C$ / (1−e$^{-k_P L}$). Using the above procedure, we can thus estimate how A_C^* and A_0^* should vary with k_P for a given L and this is shown in Fig. 1. Figure 1a shows that, as expected from theory (Field, 1983), the maximum A_C^* is indeed always observed when k_l=k_P=0.7. Also as expected, the higher the L, the greater the A_C^* at this optimum k_P. But as k_P declines (or increases) away from the optimum 0.7 value, the decline in A_C is much greater at higher L. So much so that

at k_P=0.15 and with C_C fixed (both being values which we consider typical for tropical forest of this region) A_C can actually decline with increasing L.

Figure 1b shows that changes in A_0^* that are required to satisfy Eq. (1) when C_C is conserved. As k_P increases then so does A_0^*. This occurs because the necessary gradient within the plant canopy much be sharper when k_P is greater. Likewise, at any given k_P then A_0^* is lower the greater the L. This is because the gradient in canopy photosynthetic capacity can effectively be spread over a greater depth of L. We note already at this stage that Fig. 1b implies that there are certain combinations of A_0^*, k_P and C_C which are not physiologically realistic. For example, most tropical tree species have maximum photosynthetic rates substantially less than 20 $\mu mol\, m^{-2}\, s^{-1}$ (Turner, 2001, p. 97). Thus an "optimum" k_P may not be possible – in the case of Fig. 1b unless C_C were substantially lower (see Eq. 1). But this would, however, also mean that A_C was correspondingly reduced (again as shown in Sect. 2.3). This contradiction is the fundamental reason why "optima" k_P as implied by Fig. 1a are not, in fact, optimal at all. That is to say, if one accepts that there is a fundamental limit to the maximum photosynthetic rate possible for any given species, then the "optimum" k_P requires a significantly lower canopy photosynthetic capacity were k_P to be substantially lower.

But why, despite higher canopy light interception, does A_C^* decline with increasing L at low k_P? This also turns to be critical in Sect. 2.3 in determining what is the optimum L when C_C and A_0 are taken as fixed, and the answer can be seen from Fig. 2. Here, the required gradients in A with L are shown for various combinations of k_P and L with all values standardised to A_0^* when k_l=k_P=0.7. As would be expected from Fig. 1b, when k_P<0.7 then A_0^* is also less than this "optimal case" and the greater is L; variation in photosynthetic the greater the reduction in A_0^*. The vertical variation photosynthetic losses or gains associated with $k_P \neq 0.7$ can also easily be seen by comparing the profiles for k_P=0.15 with that for k_P=0.7 and this shows that, irrespective of L, and as would be expected, that A is lower towards to top of the canopy, but that this is compensated for fully by greater A lower down. What can be seen from Fig. 2, however, is that the extent to which higher A at depth within the canopy can compensate for lower

A towards the top diminishes as L increases. As to why this occurs can be deduced from Fig. 1b. Because the high L/low k_P combination necessitates a low maximum photosynthetic capacity at the top of the canopy, much of the relatively high Q cannot be utilised. On the other hand, the extra photosynthetic capacity lower down is more or less wasted as CO_2 assimilation rates at low Q are much less dependent on $A_{max(z)}$. It is for this reason that, other things being constant, the effective reduction in A_C^* as k_P deviates from its "optimum value" increases as L increases.

It is also worthwhile pointing out at this stage that the higher the value of A_0^* the greater the relative "punishment" at any given L. This is because any removal of photosynthetic capacity away from the top of the canopy results in a proportionally greater proportional loss in A_C^* for high capacity as opposed to low capacity trees (see Fig. 1b).

2.2 What constitutes the optimal combination of L and k_P?

As argued above, due to the high A_0^* required, what is often considered the "optimum" k_P may in fact not even be physiologically possible, especially when observation based values of C_C and L are employed. Indeed, it can even be argued that for such cases the "optimality" question has previously been inappropriately posed. This is because, rather than asking what the optimum profile in photosynthetic capacity should for given values of L and C_C, one should rather be enquiring as to, given the considerable genetic and environmental limitations on A_0 that undoubtedly occur (e.g. Wright et al., 2004; Fyllos et al., 2009). "*What is the combination of L, C_C and k_P that serves to maximise the net carbon gain of the canopy for any given value of A_0*?

To achieve this, we first write

$$N_R = G_C^* - R_C - I_C\,, \tag{2}$$

where N_R is the net carbon gain to the canopy provided by the foliage on an annual basis, after accounting for the investment of carbon as new leaves within the plant canopy, (I_C) with R_C representing the annual respiratory losses by the canopy (estimated as detailed below) and G_C^* being the annual net carbon gain (Gross Primary Productivity) by

the leaves in the absence of respiration in either the dark or the light. This is the same as A_0^* but, to increase confusion, is used for calculations on an annual timescale.

Noting also that elements such as nitrogen and phosphorus which are likely to be the key modulators of variations in $A_{max(z)}$ tend to stay constant on a dry weight basis with depth within the canopy and with variations on an area being due to variations in leaf mass per unit area (M_A), see Discussion and references therein, then it then follows that we can simply express I_C as

$$I_C = I_0 e^{-k_P z}\Big|_{z=0}^{z=L} = \frac{I_0(1 - e^{-k_P L})}{k_P}, \quad (3)$$

which ends up exhibiting the interesting property of I_C not varying with k_P or L as long as C_C and A_0 are kept constant. To estimate I_0 we assume an average leaf lifetime (τ) of one year and taking typical values of M_A and carbon content for upper canopy leaves at Tapajos (88.5 g m^{-2} and 491 mg g^{-1}, respectively) obtain an estimate for I_0 of 4.5 mol C m^{-2} for an A_0 of 12 µmol m^{-2} s^{-1}. Given that there is generally little correlation between A_0 and M_A when the former is calculated on an area basis (Wright et al., 2004) we thus make I_0 independent of A_0 and for simplicities sake (and noting that it has no effect on the main conclusions of these simulations) we also make τ independent of A_{max} and I_0. A_C^* is calculated as in Eqs. (A4) and (A5) and integrated annually to obtain G_C^*, the model being driven by a dataset collected above the km87 tower at Tapajos (Goulden et al., 2004) consisting of about 3.8 years of net (incoming less reflected) Q averaged over hourly times steps and running from 1 July 2000–11 Mar 2004. Based on data of Domingues et al. (2005) night time respiration (R_n) is simply calculated as 0.08 C_C but with, importantly, daytime respiration by the leaves within the canopy dependent upon the illumination received calculated through an analysis of the data of Atkin et al. (2000) according through Eqs. (A7) or (A8) and as shown in Fig. A1b and with R_C values represent average annual sums.

Results from such a simulation are shown in Fig. 3 for our standard Tapajos conditions of A_0=12 µmol m^{-2} s^{-1} and C_C=42 µmol m^{-2} s^{-1} with k_P increased in increments

starting from a value of −0.35, with each increment sufficient to increase L by about 0.1−L being calculated in each case through a rearrangement of Eq. (1).

As k_P increases, the gradient away from the top of the canopy must by definition become sharper and, associated with this is an increase in L is required ; this being necessary to "hold" C_C within a greater leaf area. Associated with this increase in k_P and L is first an increase in G_C^* associated with an increase in light interception and with k_P approaching a similar value to k_l. Nevertheless, as L increases above a value of ∼5.4, G_C^* begins to decline. This is because of the aggravating effects of higher L on k_P/k_l imbalances as demonstrated in the previous Section (Fig. 2) outweighing any advantage of increased light interception

Although both I_C and R_n do not change with the concurrent variations in k_P and L, daytime respiration increases. This is because associated with higher L are more and more leaves at very low light levels where the inhibition of daytime respiration is considerably reduced (Fig. 1a). Thus, the net carbon gain of the canopy, I_C peaks at intermediate k_P and L, the optimum values for this simulation as being 0.123 and 4.5, respectively. These values compare surprisingly favourably with what is observed (k_P∼0.15 as discussed above with L=5.1±0.5; Aragão et al., 2005), especially because, as is discussed below, there are good reasons to think that both L and k_P should infact be a little higher than the simple estimates predicted here. We also note that an estimate for G_C^* of 262 mol C m^{-2} a^{-1} obtained from eddy covariance and other measurements at the Tapajos tower (Hutyra et al., 2007) is in remarkably good agreement with our model based estimate of G_C^* of 265 mol C m^{-2} a^{-1} at L=4.5. It is also worth noting here that although k_P<0.0 (i.e. photosynthetic capacities increasing with canopy depth) is both mathematically and physiologically possible, if is also at odds with one central tenant of the approach here (viz that A_0^* is a maximum physiologically constrained value). Thus, although included in Fig. 2. for illustrative purposes, in the simulations which follow we limit our interpretations to cases where k_P≥0.0.

2.3 What constitutes the optimal combination of A_0 and C_C?

In Sect. 2.2, we took our best estimate of the integrated canopy photosynthetic capacity for the Tapajos forest (A_0=12 µmol m^{-2} s^{-1} and C_C=42 µmol m^{-2} s^{-1}) and found, although effects of variations in L and k_P on G_C^*, R_C and N_R were relatively modest, our model optimum N_R had associated with it G_C^*, L and k_P that were surprisingly close to those actually observed. But what happens with other combinations of A_0 and C_C? To the extent that foliar nutrient concentrations are related to variations in leaf photosynthesis (Domingues et al., 2005; Mercado et al., 2009) the first should reflect some combination of genetic and environmental influences (Fyllas et al., 2009), whereas it might be reasonable to expect that C_C might be more strongly influenced by edaphic conditions or climate than genotype, this being mediated through variations in L and/or k_P.

To help answer this question, Fig. 4 therefore shows the results of simulations where we have kept the model driving Q as for Sect. 2.2, investigating now how $N_R$varies for three different photosynthetic capacities at the top of the canopy, viz A_0^*=6 µmol m^{-2} s^{-1}, 12 µmol m^{-2} s^{-1} and 18 µmol m^{-2} s^{-1} and for a variety of C_C, the range of which examined depends on the A_0^* investigated (a high A_0^*/C_C ratio leads to unreasonably high L; conversely low A_0^*/C_C lead to k_P<0.0). In all cases, the symbol plotted reflects that at the optimum N_R as determined from simulations such as given on the graph in Fig. 3, with associated k_P and L shown for selected points.

This shows that, as might be anticipated, as C_C increases from lower values, then so does N_R and that associated with this increasing N_R are reductions in the optimal k_P allowing the higher C_C to be more evenly distributed over a smaller L: the lower L reducing enhanced respiratory losses for high photosynthetic capacity leaves at the bottom of high C_C canopies. Yet, there is also a clear maximum for each A_0^*, beyond which N_R declines. This is because the enhancement in G_C^* with higher C_C increments less than the losses in R_C, including those at night. In short, above a certain point, little of the extra photosynthetic capacity can be put to good use, though still costing

the tree in terms of carbon losses.

Not surprisingly, the C_C at which this point occurs increases with A_0^*, with this being associated with a higher L and a higher k_P. For A_0^*=6 µmol m^{-2} s^{-1} the optimal prediction is no gradient in photosynthetic capacity, with a tree with such a characteristic maximising its annual carbon gain by incorporating as much photosynthetic potential into as small a leaf area as possible. As A_0^* increases the predicted "optimal" k_P increases as a partitioning resources more in-line with the light distribution assumes relatively more importance, this also being associated with a higher L. But in no case is the predicted k_P even close to that of the light extinction co-efficient (k_l=0.7 in all simulations).

2.4 Evolutionarily stable versus instantaneous model solutions

From the above, estimates of within canopy gradients in photosynthetic capacity and leaf area index are intimately interrelated, and in indeed the earliest models of canopy structure and function (Monsi and Saeki, 1953) were based on the idea that the optimal leaf area index of a canopy would be that where the lowest leaves existed at the light compensation point where daily leaf photosynthesis was just cancelled out by respiration (see also Hirose, 2005). Nevertheless, as pointed out by Anten (2002, 2005) such an calculation assumes that the optimum for an individual is not affected by the characteristics of its neighbours, being "simple optimization" in the sense of Parker and Maynard Smith (1990) This is to say, our above calculations so far have overlooked the fact that by increasing it's L above our estimated "optimum" value, a taller plant may also gain in it's chances of survival and increase its rate long term growth by shading it's neighbour(s). Looking at Fig. 4 then, one might conclude that for any given A_0^*, the "evolutionarily stable" optimal solution might, in fact, be somewhat to the left of the identified optimal value, with a slightly lower N_R and C_C. Alternatively, whilst still maintaining the same C_C it might simply increase L through an increase in k_P, as for example in Fig. 3. But what might be the magnitude of this effect? As pointed out by Anten (2002) this evolutionarily optimal L would be that where the relative losses in N_R

incurred in reducing the photosynthetic gain of one's competitors was not balanced by the relative gain in increasing their losses. In a mathematical sense then, the optimal "evolutionarily stable" L would be one where

$$\frac{dN_R}{dL} \geq -\frac{dN_C}{dL}, \quad (4)$$

with N_c representing the net carbon gain of the competitors. Computing the right hand term is difficult for such a heterogeneous systems as a tropical forest, but we have made a simple attempt of the likely effect assuming understory trees have a relatively low photosynthetic capacity of A_0^*=5 µmol m^{-2} s^{-1} with a L=1.0 and with k_P=0.15. Estimates of the upper tree "evolutionarily stable" L so calculated from Eq. (4) (denoted L°) are shown for selected combinations of A_0^* and C_C, together with L from the "individual optimization case" (Fig. 4) and a third estimate where the original Monsi and Saeki (1953) criterion is considered; viz. the L where and which the leaf at the bottom of the canopy has it's photosynthetic carbon gain exactly balanced by it's respiratory losses; in our case this "compensation point" representing the average photosynthesis and respiration rates over a 3 year period, denoted L^*.

This shows the "evolutionarily stable" L° can be as much as 3 m^2 m^{-2} greater than that calculated from Fig. 4 which is not that surprising given the only very slight reductions in N_R that occur when L increases above its optimum value (Fig. 3). Note, however, that L^* is often less than L°, and for the highest A_0^*/C_C combination, actually less than L as inferred from Fig. 4. As is noted in the discussion, this is of considerable consequence as although it is conceptually possible for a leaf at the bottom of a canopy to have a net negative carbon balance and still be a net benefit to the plant (it's costs to the plant in terms of being a net sink for carbohydrates being more than offset by it's gains to helping to shade a competitor), it seems this is not a physiologically viable possibility. This is because during leaf maturation, major physiological changes in phloem structure and physiology occur, meaning that it is impossible for adult leaves to act as net sinks of carbohydrates sourced from the rest of the plant (Turgeon, 2006), even if it were somehow in the plant's interest for them to do so. For trees with high A_0^*,

this effect occurs at much lower L (due to relatively higher respiratory costs) meaning that, despite the model as presented here initially predicting higher L with higher A_0^*, the ability for lower A_0^* trees to sustain leaves at low light levels might mean they may be able actually maintain a higher L than their faster growing counterparts (Sterck et al., 2001; Kitajima et al., 2005).

3 Materials and methods

Of a total of a total of 1508 trees sampled in 65 permanent plots in Brazil, Bolivia, Colombia, Ecuador, Peru and Venezuela between January 2002 and April 2005 for foliar nutrients and other properties (Fyllos et al., 2009; Patiño et al., 2009, 204 had also been sampled at three canopy heights for foliar nutrient composition, carbon and nitrogen isotope ratios and leaf mass per unit area (M_A). Locations, vegetation and basic soil and climatological characteristics of the sample material plots are given in Patiño et al. (2009) and Quesada et al. (2009).

3.1 Leaf sampling

Twelve to 40 trees per plot were chosen at random to collect upper canopy leaves considered to usually be exposed to the sun with the tree climber usually climbed three to eight trees in different points of the plot. From each climbed tree, braches of 1 to 2 m length from the exposed crown of two to four nearby trees were usually harvested. For randomly selected trees (generally three trees per plot) branches were additionally collected from the middle (sunny-shaded) and from the lower canopy (shaded) portion of the canopy. Sampling was achieved by severing a branch (usually ca. 4 cm in diameter) from the tree, this being subsequently allowed to fall to ground. From each branch a sub-sample was made, generally distal to the area of twig used by Patiño et al. (2008) for wood density analysis. One A4 sized plastic zip-bag of leaves of a range of possible different ages (but excluding obviously juvenile or senescencent leaves)

was then filled and sealed; kept as cool and shaded as possible and then transported to the laboratory or field station the same evening as the day of collection.

3.2 Tree and canopy height determinations

The heights of both the lowest branch and canopy of sample trees were determined using a clinometer (Model PM5/360 PC, Suunto, Turku, Finland) with "middle canopy" leaves assumed to have been at the average crown height; calculated as the arithmetic mean of the upper and lower crown dimensions.

3.3 Leaf mass per unit area (M_A)

Sub-samples of 10–20 leaves were taken for the leaves collected from each tree/measurement height combination and imaged using a locally purchased document scanner attached to a Laptop or PC. The scanned images were then saved as image files analysed and with leaf area and other associated characteristics of each images subsequently analysed using *Win Folia Basic 2001a* (Regent Instruments, Quebec, QC, Canada). Scanning was usually done on the evening of collection, but when for logistical reasons this was not possible, leaves were stored in tightly sealed plastic bags for a maximum of two days to avoid desiccation and any associated reduction of the leaf area.

Once scanned, leaves were air dried in the field or when an oven was available they were dried at 70°C for about 24 h or with a microwave oven in 5 min steps until death was considered to have been achieved. Once transported to the analysis laboratory leaves were redried at 70°C for about 24 h and their dry mass determined after being allowed to cool in a dessicator.

3.4 Sample preparation and analysis locations

Samples from Bolivia, Peru, Ecuador, Colombia and Venezuela were analysed in the Central Analytical and Stable Isotope Facilities at the Max-Planck Institute for Biogeo-

chemistry (MPI-BGC) in Jena, Germany. Samples from the Brazilian sites analysed for cations and phosphorus in at the Instituto Nacional de Pesquisas da Amazônia (INPA) in Manaus and for carbon and nitrogen in the laboratory of the Empresa Brasileira de Pesquisa Agropecuária (EMBRAPA) in Manaus. In both laboratories leaf sample not used for M_A determinations was dried as described above with a sub-sample of about 20 g DW then taken, for which the main vein of all leaves was removed and the sub-sample subsequently ground. For Brazilian leaves, sub-samples of ground material were analysed for $^{13}C/^{12}C$ ratios at the Centro de Energia Nuclear na Agricultura (CENA) in Piracicaba.

3.5 Carbon and nitrogen determinations

In both laboratories, analyses for C and N were carried out using 15–30 mg of finely ground plant material using a "Vario EL" elemental analyser (Elementar Analysensysteme, Hanau, Germany). Inter-laboratory consistency was maintained via the regular use of the same CRM 101 spruce needle (Community Bureau of Reference, BCR, Brussels, Belgium) and SRM 1573a tomato leaf (National Institute of Standards of Technology, Gaithersburg, MD, USA) standards in both laboratories. Within the Manaus laboratory, laboratory consistency with Jena values was also checked from time to time by the comparison of ground rain forest tree foliar material of various C and N concentrations already previously analysed in Jena.

3.6 Cation and phosphorus determinations

In the Jena laboratory about 100 mg of sample material was first submitted to a microwave-assisted high pressure digestion (Multiwave, Anton Paar, Graz, Austria) after addition of 3 ml of 65% HNO_3. Maximum reaction temperature was 230 °C with maximum pressures of 25–30 bar. To check for possible contamination of reagents and vessels, a blank was run with each series of standard reference materials or samples. After digestion, blank solutions and samples (reference materials and plant samples)

were transferred to 50 ml glass vessels which were filled to the mark with ultrapure water (Millipore, Eschborn, Germany) and analysed by ICP-OES (Model Optima 3300 DV, Perkin Elmer, Norwalk, CT, USA) with a 40 MHz, free-running RF-Generator and an array detector allowing for the simultaneous determination of the elements using wavelengths as given in Boumans (1987) and DIN EN ISO 11885 (1998).

In the Manaus laboratory, concentrations of P, K, Ca and Mg were determined after digestion with a nitric/perchloric acid mixture is described in detail by Malavolta et al. (1989). Concentrations of K, Ca and Mg in the extracts were subsequently determined using a Atomic Absorption Spectrophotometer (Model 1100b, Perkin Elmer, Norwalk, CT, USA) as prescribed by Anderson and Ingram (1993). Phosphorus was determined by colorimetry (Olsen and Sommers, 1982) using a UV visible spectrophotometer (Model 1240, Shimadzu, Kyoto, Japan). As for the Jena laboratory to check possible contamination of reagents and vessels, a blank was run with each series of standard reference materials or samples. Inter-calibration between the two laboratories was achieved by the use of the same external and internal standards as for C and N (Sect. 2.3).

3.7 Carbon isotope determinations

In the Jena laboratory, $^{13}C/^{12}C$ isotopes were measured as described in Werner and Brand (2001). In short: within the same sequence of analyses, bulk tissue samples, laboratory reference materials (including quality control standards) and blanks were combusted quantitatively using an NA 1110 elemental analyser equipped with an AS 128 autosampler (CE Instruments, Rodano, Italy) attached to a Delta-C isotope ratio mass spectrometer (Thermo-Finnigan MAT, Bremen, Germany) using a ConFlo III interface (Werner et al., 1999). In the CENA laboratory, Brazilian samples were analysed as described in Ometto et al. (2006). In brief, 1–2 mg of sample was combusted in an elemental analyser (CE Instruments, Rodano, Italy) coupled to an isotopic ratio mass spectrometer (IRMS Delta Plus, Thermo-Finnigan Mat, San Jose CA, USA) operating in continuous flow mode.

Inter-calibration exercises between MPI-BGC and Jena using secondary standards and other plant material showed small but significant and systematic differences between the two laboratories (r^2=0.99). These have been corrected for in the results presented here in which results from the CENA laboratory have been accordingly adjusted to provide full isotope scale equivalence with the Jena results.

4 Statistical analysis

4.1 Statistical analysis

As we were interested in vertical variations in foliar characteristics with individual trees and variations in these characteristics between individual trees as a function of canopy height (and not concerned with plot-to-plot variations – these are considered in Fyllas et al., 2009) we used multilevel modelling techniques (Snijders and Bosker, 1999) treating both tree-to-tree variation (within a plot) and variations in overall mean values (between plots) as random (residual) effects, the Basin-wide average within tree and between tree gradients being determined according to

$$\pi_{\ell tp} = \beta_{0tp} + \beta_1 h_{\ell tp} + \beta_2 h_c + R_{\ell pt}\,, \quad (5)$$

where $\pi_{\ell tp}$ can be taken to represent any physiological parameter of interest (measured on leaf "ℓ" within tree "t" located within plot "p"), β_{0tp} is an intercept term which, as indicated by its nomenclature, was allowed to vary both between trees and between individual plots, β_1 is a coefficient that describes how π varies with the height at which it was sampled (common to all leaves, trees and plots), β_2 is an additional co-efficient describing how $\pi_{\ell tp}$ varies with mean tree canopy height, h_c, and $R_{\ell tp}$ is a residual term.

The tree and plot dependent intercept can be split into an average intercept and group dependent deviations. Firstly we write

$$\beta_{0tp} = \delta_{00p} + U_{0tp}\,, \quad (6)$$

where δ_{00p} is the average intercept for the trees sampled within each plot and U_{0tp} is a random variable controlling for the effects of variations between trees (i.e. with a unique value for each tree within each plot). Likewise, we also write

$$\delta_{00p} = \gamma_{000} + V_{00p}\,, \tag{7}$$

where γ_{000} is the average intercept for the entire dataset and V_{00p} is a random variable controlling for the effects variations between each plot (i.e. with a unique value for each plot). Using a general notation then, we can combine Eqs. (5–7) to yield

$$\pi_{ltp} = \gamma_{000} + \gamma_{100} h_{\ell t} + \gamma_{010} h_c + V_{00p} + U_{0tp} + R_{\ell tp}\,, \tag{8}$$

where γ_{100} describes how variations in π between leaves within a tree vary with canopy height (with the same value for all trees within all plots) and γ_{010} is a between-tree regression coefficient that describes how π varies with the overall (mean) canopy height (with the same value applying to all trees within all plots). For the V_{00p} and U_{0tp}, just as is the case for the $R_{\ell tp}$, it is assumed they are drawn from normally distributed populations and the population variance of the lower level residuals ($R_{\ell t}$) is likewise assumed to be constant across trees. Note that within each plot the mean value of $U_{0tp} \equiv 0$ and likewise the mean value of $V_{0tp} \equiv 0$ for the dataset as a whole. As is the normal case in any regression model, within each tree the mean $R_{\ell tp} \equiv 0$.

Equation (8) is a "three-level random intercept model" with leaves (level 1) nested within trees (level 2) which are themselves nested within plots (level 3). Associated with the three residual terms there is variability at all three levels and we denote the associated variances as

$$\mathrm{var}(R_{\ell tp}) = \sigma^2, var(U_{0tp}) = \tau^2, \mathrm{var}(V_{00p}) = \phi^2\,. \tag{9}$$

The total variance between all leaves is $\sigma^2+\tau^2+\phi^2$ and the population variance between trees is $\tau^2+\phi^2$.

Equation (8) is flexible in that the within-tree regression coefficient is allowed to differ from the between-tree regression coefficient. In analogy with the two-level model

derivation in Chap. 4 of Snijders and Bosker (1999) considering the terms within a given tree, the terms can be reordered as

$$\pi_{\ell tp} = (\gamma_{000} + \gamma_{010} h_c + U_{0t} + V_{00p}) + \gamma_{100} h_{\ell tp} + R_{\ell tp} . \quad (10)$$

The random part between the parenthesis is the intercept for this tree and the regression coefficient for variation of π with height within trees is γ_{100}. The systematic (non-random) part is the within-tree regression line

$$\pi_{\ell tp} = (\gamma_{000} + \gamma_{010} h_c) + \gamma_{100} h_{\ell tp} . \quad (11)$$

On the other hand, considering only the relationship between the average value of π within a canopy and the average canopy height, h_C, then Eq. (10) becomes

$$\pi_{.tp} = \gamma_{000} + \gamma_{010} h_c + \gamma_{100} h_c + V_{00p} + U_{0tp} , \quad (12)$$

and the systematic part of the model can then be written as

$$\pi_{.tp} = \gamma_{000} + (\gamma_{010} + \gamma_{100}) h_c . \quad (13)$$

This shows that the between-tree regression coefficient is the random intercept model is $\gamma_{010}+\gamma_{100}$. Thus in the analysis which follows, when the relationship between any parameter π and height is different for between tree as opposed to within-tree variation then γ_{010} is significantly different from zero. Where this is not the case, any variation in π with height is of a statistically similar magnitude irrespective of whether or not the source of variation is sampling at different heights within the one tree or comparing the average values for trees of different heights. All analyses were undertaken with the *MLwinN* software package (Rabash et al., 2004). Heights were centred according to the mean tree height for the dataset (19.8 m) so the intercept estimates (γ_{100}) represent the estimated value of each π at that height.

5 Results

5.1 Sources of variation

In order to examine the inherent sources of variability in the dataset, we first fitted a "null model" to untransformed data according to

$$\pi_{\ell t} = \gamma_{00} + V_{00p} + U_{0tp} + R_{\ell tp} \,. \quad (14)$$

From this model and Eq. (9) the contribution of variations within and between trees and plots to the overall variance within the dataset can be simply apportioned and the results are shown in Fig. 5. This shows that, without exception, the variability observed in the eight π examined (M_A and $\delta^{13}C$, with N, P, C, Ca, K and Mg on a dry weight basis) was greater between trees than the variance associated with the sampling of the three different heights within trees. Moreover, the between-plot variance was also generally less than the within-plot (between tree) variance.

5.2 Vertical profiles

The underlying raw data giving rise to Table 2 and used in the subsequent multilevel analysis is shown for M_A, $[N]_{DW}$, $[P]_{DW}$, $[C]_{DW}$, $\delta^{13}C$ and $[Mg]_{DW}$ in Fig. 6, with colours coding for the different regions. This shows that, although there is considerable variability in the data, certain patterns exist. For example, on average there is a trend for am increase in M_A with h and the opposite is the case for $\delta^{13}C$. On the other had, generally speaking concentrations in $[N]_{DW}$ and $[P]_{DW}$ are quite consistent within a given tree, although there are of course exceptions, especially at higher concentrations. Foliar C varies substantially between trees, and close examination shows that although usually very consistent within a given tree, there is often a slight tendency for [C] to increase with height. Variations in $[Mg]_{DW}$ were similar to $[Ca]_{DW}$ and $[K]_{DW}$ with no strong trend with height apparent.

BGD
6, 4639–4692, 2009

From Fig. 6 there is considerable heteroscedastity in the data with the variance of the dependent variables tending to increasing with their absolute value but independent of the value of the independent (height variable). This was the case for all π except maybe C and δ^{13}C. Moreover, an examination of residual variances showed marked departures from normality, even when plot-to-plot differences in overall mean values were taken into account. We therefore transformed all data (taking the absolute value of δ^{13}C) prior to analysis, fitting the equation

$$\log_e(\pi_{\ell tp}) = \gamma_{00} + \gamma_{10} h_{\ell t} + \gamma_{01} h_c + V_{00p} + U_{0tp} + R_{\ell tp} \,. \quad (15)$$

Results are listed in Table 2, for which the null hypothesis that a certain regression parameter (γ_h) is zero (i.e. H_0: γ_h=0) can be tested according to (") (two tailed t-test $T(\gamma_h)=\hat{\gamma}_h/[S.E.(\hat{\gamma}_h)]$, the so called *Wald test*. This indicates (as shown in bold font) that within tree canopy gradients were significantly different to zero only for M_A, $[C]_{DW}$, δ^{13}C and $[Mg]_{DW}$. From Eq. (13), the parameter γ_{010} reflects the difference between the within-tree and between-tree slopes but a separate Wald test can be used to determine if the overall co-efficient for the between tree coefficient ($\gamma_{100}+\gamma_{010}$) is significantly different from zero (Snijders and Bosker, 1999). From such an analysis we can conclude

1. The between tree coefficient for M_A is not significantly different to the within tree co-efficient and both show M_A are significantly different to zero. Both increase with increasing height.

2. There is no detectable within-tree gradient for nitrogen, phosphorus of calcium when expressed on a dry-weight basis. Nor is overall, there any significant overall tendency for mean canopy nitrogen or phosphorus concentrations to increase with mean canopy height.

3. Foliar $|\delta^{13}C|$ decreases with height irrespective of whether the source of variation is within-tree or between tree. That is to say, taller trees have less negative δ^{13}C than shorter trees and lower leaves also tend to have less negative δ^{13}C than

higher leaves within the same tree. The gradients with height are similar for both sources of variation and are both significantly different from zero.

4. There is a significant tendency for $[C]_{DW}$ to increase with height within an individual tree, and also for taller trees to have a higher foliar C content.

5. Although there is a significant tendency for $[Mg]_{DW}$ to decrease with increasing height within a given tree, the opposite pattern is observed for the variation between trees. Taller trees tend to have significantly higher $[Mg]_{DW}$ than shorter ones. Potassium also shows a significant tendency to decrease with increasing height within a given tree, but, contrary to magnesium with this effect perhaps being amplified, rather than reversed, when tree-to-tree variation is considered.

Figure 7 shows the fitted slopes and the data, in all cases normalised to the fitted value for each tree at the average sampling height of 19.8 m. Here a comparison of the plots for within-tree and between-tree variation show the generally similar increases for M_A with height and in decreases $\delta^{13}C$ and $[C]_{DW}$ with height, irrespective of the source of variation. On the other hand, the much steeper gradient for $[K]_{DW}$ when between-tree variations are considered is also apparent as the strong contrast in directions for $[Mg]_{DW}$. Taller trees tend to have higher $[Mg]_{DW}$, but within individual trees $[Mg]_{DW}$ declines with height. Though not significant, the trends for slightly decreased [N] and [P] with height in individual tree canopies can also clearly be seen.

5.3 Area based profiles

Vertical variations [N] and/or [P] within canopies can be expected to substantially influence tropical forest canopy photosynthetic rates which are normally expressed per unit leaf area (Carswell et al., 2000; Domingues et al., 2005; Mercado et al., 2009), and it is also thus of interest to examine vertical gradients within and between trees also expressing nutrients on a leaf area basis (Table 3) – this simply being calculated as the product of the nutrient concentration (DW basis) and M_A. When done, this shows

similar and significant positive gradients to exist for both nitrogen $[N]_A$) and phosphorus $[P]_A$) and, although not significantly different, the between tree gradients are in both cases about 50% steeper than the within-tree gradients. The negative gradient in C_A as on a DW basis is maintained, as is the positive gradient for K_A, though in the case of K_A the between-tree gradient is no longer statistically stronger than observed within individual trees. The pattern for magnesium is also very different on leaf-area versus dry-weight basis. The negative DW gradient (lower values higher up in the canopy) is counterbalanced by the positive gradient in M_A meaning that within individual tree canopies no gradient in Mg exists. On the other hand, the positive between-tree gradient in magnesium is amplified when expressed on an area basis.

Leaf area based gradients for nitrogen and phosphorus are shown in Fig. 8, again with each tree having its value normalised to the fitted value at the average sampling height of 19.8 m This illustrates the similar overall patterns observed for N_A and P_A, a result that is not surprising as a comparison of Fig. 8 with Fig. 7 in conjunction with Tables 2 and 3 shows that almost all the variation observed in N_A and P_A; both within and between trees is due to the increase in M_A with height with $[N]_{DW}$ and $[P]_{DW}$ on a dry weight basis varying little with height and with $[N]_{DW}$ perhaps even decreasing slightly. From a consideration of measured average leaf area indices of the canopies examined (ca. 5.4; Patiño et al., unpublished) in conjunction with the average canopy depth as measured by the differences in height between the top of the tallest and the bottom of the lowest trees, we estimate that the average combined within/between tree gradient for the forests examined would relate to an extinction coefficient when expressed as a function of cumulative leaf area index (as per the accompanying model simulations in this paper, k_P) of only around 0.10. Nevertheless, such a calculation is necessarily rough as it involves assumptions about the relative contribution of within-tree versus between-tree gradients to that observed across the canopy overall.

5.4 Do tree-to-tree variations in within-canopy gradients exist?

The analysis so far has assumed that the within-tree gradients are the same for all sites and trees, but that different sites and the trees within them trees may assume different overall nutrient concentrations (a "random intercept model") But, especially in light of the model results of Sect. 2, it is also of interest to determine if the gradients really do differ between trees, and if so, in a systematic way. Given the "noise" apparent in Fig. 6, this is obviously not an easy question to answer, but it can be tested by taking $\beta_{1tp}=\gamma_{100}h_{\ell tp}+U_{1tp}h_{\ell tp}$ (see Eq. 5), this then adding an additional random term to Eq. (8) viz,

$$\pi_{\ell tp} = \gamma_{000} + \gamma_{100}h_{\ell tp} + \gamma_{010}h_c + V_{00p} + U_{0tp} + U_{1tp}h_{\ell tp} + R_{\ell tp}\,. \quad (16)$$

The additional term allows different trees to have different within-canopy gradients – a so called "random slope model" (Snijders and Bosker, 1999) with a χ^2 test then employable to see if the model fit has been improved. And indeed, when this was attempted, it was found that significant tree-to-tree variation in within canopy gradients was observed for M_A, $|\delta^{13}C|$ and P_A (but not for $[N]_A$). Moreover, as is shown in Fig. 9 these variations in slopes (or "extinction coefficients") were not random, but inter-related and correlated with the mean M_A, $|\delta^{13}C|$ and P_A of the trees concerned. In particular, all three were well correlated with mean canopy P_A, this being the average of all three measurements taken on each tree, denoted $\langle[P]_A\rangle$, with the very similar patterns for the gradients in M_A and P_A with $\langle[N]_A\rangle$ suggesting that most of the between tree variability in within canopy gradients in P_A was due to variations in M_A rather than $[P]_{DW}$. The strong decline in $|\delta^{13}C|$ with increasing $\langle[P]_A\rangle$ is also of note, suggesting that variations in ^{13}C discrimination within the canopy of trees are intricately linked with plant metabolic processes.

BGD
6, 4639–4692, 2009

6 Discussion

That plants can acclimate to different light levels at chloroplast, leaf and canopy has long been appreciated (Monsi and Saeki, 1953; Boardman, 1977; Björkman, 1981) and a key focus of recent years has been understanding the way plants that allocate their resources throughout their canopies, with one key focus being photosynthetic carbon gain (Niinemets, 2007). It was Field (1983) who first proposed that plant photosynthetic carbon gain would be optimized if key physiological resources required for photosynthesis (in his case nitrogen) were allocated in direct proportion to the par received. This idea of "optimization" is conceptually attractive with this assumption even being incorporated into some canopy gas exchange models (Lloyd et al., 1995; Sands, 1995; Sellers et al., 1996). But it is also now clear that although the decline in photosynthetically important elements such as nitrogen and phosphorus within plant canopies can be considerable and even impressive, this is never to the same degree that it matches the decline in the light environment (De Jong and Doyle, 1985; Carswell et al., 1980; Meir et al., 2002; Anten 2005; Wright et al., 2006).

As to why this should be so has proved somewhat of an enigma, it being generally accepted that natural selection should have resulted in plants optimising their resource strategies and various hypotheses have been proposed to account for this apparent "non-optimality". These include the fact that plants do not grow as isolated individuals with bur rather in competition with others (Anten, 2005), that it might be related to direct versus diffuse radiative transfer (Alton and North, 2007) or not all nitrogen being related to photosynthesis (Hikosaka, 2005); that there may be optimisation of N to light gradients within leaves as well as canopies (Terashima et al., 2005); that the required high very nitrogen concentrations at the top of the canopy may place leaves at strong risk of herbivory (Stockhoff, 1994); that there may be considerable costs of retranslocating nutrients within the plant (Wright et al., 2006) that plants may overinvest in Rubisco in order to cope with temporal vicariates in the environment (Warren et al., 2000) and, especially as gradients in nutrients and photosynthetic capacity are

generally driven by gradients in M_A rather dry-weight variations (Reich et al., 1998; Evans and Poorter, 2001) that there may be a practical lower limit to the minimum M_A and hence N_A that any species can achieve (Meir et al., 2002).

Though with some affinity with the latter the suggestion, the answer we present to this long standing apparent discrepancy differs to other suggestions made to date. That is to say: The optimality question has actually been incorrectly posed. And we suggest from our simulations and results presented here that once correctly posed, it turns out gradients of photosynthetic resources within plant canopies are, in fact, close to optimal.

For example, in some cases it has simply been assumed that the problem is simply one of allocating resources for a canopy of a given leaf area index and photosynthetic capacity (as observed). But when this is done (e.g. dePury and Farquhar, 1995) what emerges are unrealistically high nutrient concentrations being required at the top of the canopy, inconsistent with the physiological tradeoffs that clearly exist in terms of leaf structure and function (Wright et al., 2004). This is similar to the point of Meir et al. (2002) already mentioned above, that there is probably also a realistic lower limit to the M_A and nutrient content that any species can attain.

Although flexibility no doubt exists it also is now well established that different species have different characteristic maximum values of M_A, [N] and [P] (Fyllas et al., 2009), this being closely linked to other aspects of their physiological strategy including leaf lifespans (Wright et al., 2004) and hydraulic characteristics (Santiago et al., 2004; Patiño et al., 2009). Thus the optimisation question should also be viewed within the constraints of these known physiological boundary conditions such as the maximum (species dependent) photosynthetic potential of the leaves at the top of the canopy, and, in some cases, the practical minimum value achievable at the bottom of the canopy, this perhaps being structural (as suggested by Meir et al., 2002), or alternatively being a consequence of the need for all leaves to maintain a positive carbon balance once mature (Turgeon, 2006), as discussed in Sect. 2.4.

One simple way to view the argument and it's consequences it is through following

the individual lines shown in Fig. 4. A plant with an "optimal" distribution of it's photosynthetic resources (high k_P) unavoidably has less photosynthetic resources than one that does not (low k_P). Thus, it is actually to a plants advantage to have a shallow gradient in photosynthetic resources as this allows it to have a greater overall photosynthetic capacity (C_c) and hence a higher net rate of carbon gain, N_R. As discussed in Sect. 2.4, it turns out there are several complexities which end up influencing the minimum k_P and maximum N_R which should occur, but nevertheless, the theory and model as presented here does lead to the (intuitive) prediction that plant with a low overall photosynthetic capacities should have shallower gradients in their photosynthetic resources than those with higher photosynthetic capacities. This can be inferred, for example, if we accept that phosphorus has a role in the photosynthetic process for tropical tress (Raaimakers et al., 1995; Lloyd et al., 2001) from the relationship between $\langle[P]_A\rangle$ and the gradients shown in Fig. 9. It is also consistent with greater differences between sun and shade leaves in M_A and many other leaf characteristics (including P_A) for gap-dependent species (as opposed to obligate-gap species or gap-independent species) observed by Popma et al. (1992) for a tropical forest in Mexico, with the gap-dependent species also having higher N_A and P_A a than the other two species groups.

As is evidenced from Fig. 8 this tree-to-tree variation in the gradients in M_A and P_A are also accompanied by correlated variations in $\delta^{13}C$, this suggesting that that for such trees compensating gradients in stomatal conductances do not necessarily occur.

Gradients in height were also observed in plant carbon contents, both within and between trees. Small within canopy gradients in $[C]_{DW}$ have been reported before by Poorter et al. (2006) who accounted for lower construction costs of low irradiance leaves in terms of lower levels of soluble phenolics. Studying upper-canopy leaves from across the Amazon Basin, Fyllas et al. (2009) also observed significant variations in foliar carbon content, relating this to variations in M_A and the extent of investment in constitutive defences.

Consistent with this and the observed positive vertical gradient in between and within

trees is the tendency for leaves higher up rain forest canopies to have greater levels of carbon based defence compounds (Lowman and Box, 1983; Downum et al., 2001; Dominy et al., 2003), this perhaps being associated with higher abundances of herbivores such as insects and other arthropods also occurring there (Sutton, 1989; Kato et al., 1995; Koike et al., 1998; Basset et al., 2001).

The decrease in $[Mg]_{DW}$ with height within individual trees (Table 2, Fig. 7) seems similar to that reported by Grubb and Edwards (1982) comparing saplings and mature trees within a New Guinea montane rain forest. They attributed this to the central role of Mg within the chlorophyll (Chl) complex (Shaul, 2002) with increased $[Chl]_{DW}$ for shaded leaves being a well documented phenomenon (Boardman, 1977; Björkman, 1981) – as generally seems to be also the case for tropical forest trees (Rozendaal et al., 2006). The intra-tree Mg gradient was not, however, significant when expressed on a leaf area basis, despite both $[N]_A$and $[P]_A$ declining with increasing canopy depth. Particularly for N this is consistent with the idea that in shaded conditions a large portion of N is invested in chlorophyll for light capture, leading to a high Chl:N ratios. On the other hand, for light exposed leaves a large proportion of N is invested in Rubisco with commensurate low Chl: N ratios (Poorter et al., 2000; Evans and Poorter, 2001). On the other hand, it was also found that $[Mg]_A$ increased with height along with $[N]_A$and $[P]_A$ when inter-tree differences in tree height were the source of vertical variation (Table 3), even though when comparing different rain forest trees $[Chl]_A$ seems to be independent of light environment or tree height (Rijkers et al., 2000). Probably then, this increase in $[Mg]_A$ with tree height relates to its other physiological functions, for example in the process of thylakoid acidification (Pottosin and Schönkmecht, 1996), as an activator of several photosynthetic enzymes including Rubisco (Gardemann et al., 1986; Portis, 1992) and as a ATP-cofactor required for phloem loading of sugars (Shaul, 1992). All these physiological functions would be expected to need to be proceeding at higher rates in taller trees with higher $[N]_A$ and $[P]_A$. This is because such trees would also most likely also have a higher photosynthetic rates by virtue of greater A_{max} (associated with higher $[N]_A$ and $[P]_A$) as well as a greater probability of high light

interception compared to trees occurring lower down the canopy stratum.

Appendix A

Gradients of photosynthetic capacity in plant canopies

As shown by Field (1983) the photosynthetic rate of a canopy of a given leaf area index (L) and Q_0 is the incident photon irradiance at the top of the canopy photosynthetic capacity should be maximised if throughout that canopy nitrogen, or any other factor considered to be limiting for photosynthesis was distributed in direct proportion to the photon irradiance (Q). A similar situation exists for the photosynthetic machinery of leaves (Farquhar, 1989). Although conceptually attractive in terms of an optimisation of valuable resources and as a tool for modelling studies (Lloyd et al., 1995; Haxeltine and Prentice, 1996; Sellers et al., 1996), numerous field observations have shown this not, infact be the case. Gradients of nitrogen in particular are generally less than those predicted by the Field (1983) model (Meir et al., 2002; Wright et al., 2006). Here we show why this should be the case.

We first start with a general equation describing the photosynthesis the light dependence of photosynthesis, the rectangular hyperbola, viz:

$$A_z = \frac{A_{\max(z)} \phi Q_z}{A_{\max(z)} + \phi Q_z} - R_z \,, \tag{A1}$$

where A_z represents the net CO_2 assimilation rate of a leaf at some point, z, within the canopy, $A_{\max(z)}$ is the maximum net CO_2 assimilation rate of the leaf in question (at light saturation), ϕ is the quantum yield, Q_z is the photon irradiance at the leaf surface and R_z is the rate of respiration by the leaf. Equation (A1) is of a slightly different form to that of a rectangular hyperbola usually presented (Causton and Dale, 1990), allowing a constant ϕ (independent of $A_{\max(z)}$). From both empirical and functional points of view better equations exist, for example the monomolecular (Causton and

Dale, 1990) or hyperbolic minimum functions (Farquhar et al., 1980). But unfortunately, both equations lead to intransigent integrals when applied in the approach shown below (see also Buckley and Farquhar, 2004).

We first ignore respiration, allowing both A_{max} and Q to decline exponentially through the canopy according to

$$A_{max(z)} = A_0 e^{-k_P z}; \quad Q_z = Q_0 e^{-k_l z}, \tag{A2}$$

where A_0 is the maximum (light saturated) photosynthetic rate of the leaves at the top of the canopy, k_P is an "extinction" coefficient describing the decline in photosynthetic capacity, k_l is an "extinction" coefficient describing the decline in photon irradiance and. A combination of Eq. (A1) and (A2) when integrated downwards through a canopy of leaf area index L is

$$A_C^* = \int_0^L \frac{A_0 e^{-k_P z} \varphi Q_0 e^{-k_l z}}{A_0 e^{-k_P z} + \varphi Q_0 e^{-k_l z}_l} dz. \tag{A3}$$

Where A_C^* is the photosynthetic rate of the canopy, ignoring any respiration in the light. An analytical solution to Eq. (A3) exists, being

$$A_C^* = \frac{A_0(k_l - k_P)e^{-kiz} - F_1\left[k_P/(k_P - k_l), 1, (2k_P - k_l)/(k_l - k_P), -A_0 e^{(k_l - k_P)z}/(\varphi Q_0)\right]}{k_P}\Bigg|_{z=0}^{z=L}. \tag{A4}$$

Here ${}_2F_1\,[a, b, c, \zeta]$ is Gauss's hypergeometric function (Abramowitz and Stegun, 1972) which can be estimated numerically, for example using the algorithm of Forrey (1997). When k_P=k_l then Eq. (A4) is undefined, but calculation is still possible as for this special case

$$A_C^* = \frac{-A_0 \varphi Q_0 e^{-k_l z}}{k_l(A_0 + \varphi Q_0)} = \Bigg|_{z=0}^{z=L} \frac{A_0 \varphi Q_0 (1 - e^{-k_l L})}{k_l(A_0 + \varphi Q_0)}. \tag{A5}$$

Note that Eq. (A5) is very similar in form to Eq. (A1) with the term $(1-e^{-k_l L})/k_l$ representing the co-ordinated decline of both light and photosynthetic capacity down the canopy.

A respiration term can be now be added to Eq. (A4) or Eq. (A5). We first take the result of Atkin et al. (2000) who showed for *Eucalyptus pauciflora* who showed at 30°C the rate of respiration in the light first rapidly declines with irradiance, then subsequently increases at a much slower rate. From their data, we therefore fitted a curve of the form

$$R_z = R_{d(z)}\left(1 - \frac{\alpha Q_z}{\beta + Q_z} + \gamma Q_z\right), \quad \text{(A6)}$$

where R_d is the (maximum) rate of foliar respiration in the dark and with α, β and γ being fitted constants with values of 0.9575, 29.85 μmol m^{-2} s^{-1} and 5.114×10^{-5} μmol quantaμmol^{-1} CO_2, respectively (r^2=0.999). This is shown in Fig. 1a.

Numerous studies have shown that leaf respiration rates in the dark tend to scale with variations in photosynthetic capacity, this also being the case for tropical forests (Domingues et al., 2005). We can therefore express R_d as a constant fraction, f, of A_{max}, a typical value of which is 0.08, although this fraction may decline to some extent with depth within the canopy (Cavaleri et al., 2008). Light response curves for a range of $A_{max(z)}$ and with f=0.08 are shown in Fig. 1b (Eq. A1 combined with Eq. (A6) and with $R_{d(z)}$=0.08$A_{max(z)}$).

Light response curves for a range of $A_{max(z)}$ combined with Eq. A2 gives

$$R_C = \left.\frac{fA_0 e^{-(k_P-k_l)z}\left\{\begin{array}{c} Q_0\alpha k_P - (k_P+k_l)\beta e^{k_l z} + \gamma_2 Q_0 k_P) \\ -{}_2F_1\left[1,(k_P-k_l)/k_P,-k_P/k_l,-\beta e^{k_l z}/Q_0\right]\end{array}\right\}}{\beta k_P/(k_P-k_l)}\right|_{z=0}^{z=L}. \quad \text{(A7)}$$

As for Eq. (A4), we can also express Eq. (A6) in an alternative and simpler form for the special case of $k_P = k_l$ viz

$$R_C = fA_0 \left(\frac{(\alpha - 1)e^{-k_l z}}{k_l} - \frac{Q_0 \gamma e^{-2k_l z}}{2k_l} - \frac{\alpha\beta \log_e[\beta + Q_0 e^{-k_l z}]}{Q_0 k_l} \right) \Bigg|_{z=0}^{z=L} . \quad \text{(A8)}$$

In all simulations presented here, Eq. (A6) has been subtracted from Eq. (A4) (or (A7) subtracted from Eq. (A5)) to give a net CO_2 assimilation rate, $A_C = A_C^* - R_C$ with the hypergeometric functions solved using the algorithm of Forrey (1997). When applying this algorithm if was found, however, that as $k_P \rightarrow k_l$ that sometimes the numerical solution did not converge, especially at low light as where ζ could be strongly negative and a and c took on large values for the hypergeometric function in Eq. (A4). For such cases, we therefore substituted a representation of a continued equation form of the hypergoemetric function which for most of the offending combinations of a, b and z did allowed a stable solution to be obtained. Here we used the general approach of Lenz (1976) as modified by Thompson and Barnett (1986).

References

Abramowitz, M. and Stegun, I. A.: Hypergeometric Functions, in: Handbook of Mathematical Functions with Formulas, Graphs, and Mathematical Tables, 9th edn., New York, Dover, 555–566, 1972.

Alton, P. B. and North, P.: Interpreting shallow, vertical nitrogen profiles in tree crowns: A three-dimensional, radiative-transfer simulation accounting for diffuse sunlight, Agr. Forest Meteorol., 145, 110–124, 2007.

Anderson, J. M. and Ingram, J. S. I.: Tropical Soil Biology and Fertility: A Handbook of Methods, CAB International, Oxford, 1989.

Anderson, J. M. and Ingram, J. S. I.: Tropical soil biology and fertility: a handbook of methods, CAB International, Wallingford, UK, 1–221, 1993.

Anten, N. P. R.: Evolutionarily stable leaf area production in plant populations, J. Theor. Biol., 217, 15–32, 2002.

Anten, N. P. R.: Optimal photosynthetic characteristics of individual plants in vegetation stands and implications for species coexistence. Ann. Botan. 95, 495–506, 2005
Atkin, O. K., Evans, J. R., Ball, M. C., Lambers, H., and Pons, T. L.: Leaf respiration of snow gum in the light and dark. interactions between temperature and irradiance, Plant Physiol., 122, 915–923, 2000.
Aragão, L. E. O. C., Shimabukaro, Y. E., Santo, F. D. B. E., and Williams, M.: Landscape pattern and spatial variability of leaf area index in Eastern Amazonia, Forest Ecol. Managem., 211, 240–256, 2005.
Basset, Y., Aberlenc, H.-P. Barrios, H., Curtelli, G., Bérenger, J.-M., Vesco, J.-P., Causse, P., Haugm A., Hennion, A.-S., Lescobre, L., Marques, F., and O'Meara, R.: Stratification and diel activity of arthropods in a lowland rainforest in Gabon, Biol. J. Linn. Soc., 72, 585–607, 2001.
Björkman, O.: Responses to different quantum flux densities, Encyclopedia of Plant Physiology, 12, 57–107, 1981.
Boardman, N. K.: Comparative photosynthesis of sun and shade plants, Annu. Rev. Plant Phys., 28, 355–377, 1977.
Boumans, P. W. J. M.: Inductively Coupled Plasma Emission Spectrometry: Part I, John Wiley & Sons, New York, 1987.
Buckley, T. N. and Farquhar, G. D.: A new analytical model for whole-leaf potential electron transport rate, Plant Cell Environ., 27, 1487–1502, 2004.
Carswell, F. E., Meir, P., Wandelli, E. V., Bonates, I. C. M., Kruijt, B., Barbosa, E. M., Nobre, A. D., Grace, J. and Jarvis, P.G.: Photosynthetic capacity in a central Amazonian rain forest, *Tree Physiol.*, 20, 179–186, 2000.
Causton, D. R. and Dale, M. P.: The monomolecular and rectangular hyperbola as empirical models of three Veronica species, Ann. Bot-London, 65, 389–394, 1990.
Cavaleri, M., Oberbauer, S. F., and Ryan, M. G.: Foliar and ecosystem respiration in an old growth tropical forest. Plant Cell Environ., 31, 473–483, 2008.
Chen, J. J., Reynolds P., Harley P., and Tehnunen, J.: Coordination theory of nitrogen distribution in a canopy, Oecologia, 93, 63–69, 1993.
Cromer, R. N., Kriedemann, P. E., Sands, P. J., and Stewart, L. G.: Leaf growth and photosynthetic response to nitrogen and phosphorus in seedling trees of Gmelina arborea, Austral. J. Plant Physiol., 20, 83–98, 1993.
DeJong, T. M. and Doyle, J. F.: Seasonal relationships between leaf nitrogen content (pho-

tosynthetic capacity) and leaf canopy light exposure in peach (Prunus persica), Plant Cell Environ., 8, 701–706, 1985.
De Pury, D. G. G. and Farquhar, G. D.: Simple scaling of photosynthesis from leaves to canopies without the errors of big-leaf models, Plant Cell Environ., 20, 537–557, 1997.
DIN EN ISO 11885: Determination of 33 elements by inductively coupled plasma atomic emission spectroscopy, Brussels: European Committee for Standardization, 1998.
Domingues, T. F., Berry, J. A., Martinelli, L. A., Ometto, J. P. H. B., and Ehleringer, J. R.: Parameterization of canopy structure and leaf-level gas exchange for an Amazonian tropical rain forest (Tapajós National Forest, Pará, Brazil). Earth Interactions, 9, Paper No. 17, 2005.
Dominy, N. J., Lucas, P. W., and Wright, S. J.: Mechanics and chemistry of rain forest leaves; canopy and understory compared, J. Exp. Bot., 54, 2007–2014, 2003.
Downum, K., Lee, D., Hall, F., Quirke, M., and Towers, N.: Plant secondary compounds in the canopy and understory of a tropical rainforest in Gabon, J. Trop. Ecol., 17, 477–481, 2001.
Evans, J. R.: Photosynthesis and nitrogen relationships in leaves of C_3 plants, Oecologia, 78, 9–19, 1989
Evans, J. R. and Poorter, H.: Photosynthetic acclimation of plants to growth irradiance: the relative importance of specific leaf area and nitrogen partitioning in maximizing carbon gain, Plant Cell Environ., 24, 755–767, 2001.
Farquhar, G. D., Caemmerer, S., and Berry, J. A.: A biochemical model of photosynthetic CO_2 assimilation in leaves of C_3 species, Planta, 149, 78–90, 1980.
Farquhar, G. D.: Models of integrated photosynthesis of cells and leaves, Philosophical Trans. Roy. Soc. London. Series B, Biological Sciences, 357–367, 1989.
Field, C. B.: Allocating leaf nitrogen for the maximisation carbon gain: leaf age as a control on the allocation program, Oecologia, 56, 314–347, 1983.
Field, C. B. and Mooney, H. A.: The photosynthesis-nitrogen relationship in wild plants, in: The Economy of Plant Form and Function (T. J. Givnish, ed.), Cambridge University Press, Cambridge, 25–55, 1986.
Forrey, R. C.: Computing the hypergeometric function, J. Comp. Phys., 137, 79–100, 1997.
Fyllas, N. M., Patiño, S., Baker, T. R., Nardoto, G. B., Martinelli, L., Quesada, C. A., Paiva, R., Schwarz, M., Horna, V., Mercado, L. M., Santos, A. J. B., Arroyo, L., Jiménez, E. M., Luizão, F. J., Neill, D. A., Silva, N., Prieto, A., Rudas, A., Silviera, M., Viera, I., Lopez-Gonzalez, G., Malhi, Y., Phillips, O. L., and Lloyd, J.: Basin-wide variations in foliar properties of Amazon forest trees: Phylogeny, soils and climate, Biogeosciences, accepted, 2009.

Gardemann, A., Schimikat, A., and Heldt, H. W.: Control of CO_2 fixation: Regulation of stromal fructose-1,6-bisphosphate in spinach by pH and Mg^{2+} concentration, Planta, 168, 536–545, 1986.

Goulden, M. L., Miller, S. D., da Rocha, H. R., Menton, M. C., de Freitas, H. C., Figueira, A. M. E. S., and de Sousa, C. A. D.: Diel and seasonal patterns of tropical forest CO_2 exchange, Ecol. Appl., 14(4), S42–S54, 2004.

Grubb, P. J. and Edwards, P. J.: Studies of mineral cycling in a montane rain forest in New Guinea III. The distribution of mineral elements in the above-ground material, J. Ecol., 72, 623–648, 1982.

Hallé, F., Oldeman, R. A. A., and Tomilson, P. B.: Tropical Trees and Forests. An Architectural Analysis, Springer-Verlag, Berlin, 1978.

Haxeltine, A. and Prentice, I. C.: A general model for the light-use efficiency of primary production, Funct. Ecol., 10, 551–561, 1996.

Hikosaka, K.: Leaf canopy as a dynamic system: ecophysiology and optimality in leaf turnover, Ann. Bot.-London, 95, 521, 2005.

Hirose, T.: Development of the Monsi-Saeki theory on canopy structure and function, Ann. Bot.-London, 95, 483, 2005.

Hollinger, D. Y.: Optimality and nitrogen allocation in a tree canopy, Tree Physiol., 16, 627–634, 1996.

Hutyra, L. R., Munger, J. W., Gottlieb, E. W., Daube, B. C., Camargo, P. B., and Wofsy, S. C.: Seasonal controls on the exchange of carbon and water in an Amazonian rainforest, J. Geophys. Res., 112, G03008, doi:10.1029/2006JG000365, 2007.

Jarvis P. G., James, B. G., and Landsberg, J. J.: Coniferous forest, in: Vegetation and Atmosphere, edited by: Monteith, J. L., Academic Press, London, 171–204, 1976.

Kato, M., Inoue, T., Hamid, A. A., Nagamitsu, T., Merdek, M. B., Nona, A. R., Itino, T., Yamane, S., and Yumoto, T.: Seasonality and vertical structure of light-attracted insect communities in a Dipterocarp forest in Sarawak, Res. Popul. Ecol., 37, 59–79, 1995.

Kitajima, K., Mulkey, S. S., and Wright, S. J.: Variation in crown light utilization characteristics among tropical canopy trees, Ann. Bot.-London, 95, 535–547, 2005.

Koike, F., Riswan, S., Partomihardjo, T., Suzuki, E., and Hotta, M.: Canopy structure and insect community distribution in a tropical rain forest of West Kalimantan, Selbyana, 19, 147–154, 1998.

Kull, O. and Niinemets, U.: Distribution of photosynthetic properties in leaf canopies; compari-

son of species with different shade tolerance, Funct. Ecol., 12, 472–479, 1998.
Lentz, W. J.: Generating Bessel functions in Mie scattering calculations using continued fractions, Applied Optics, 15, 668–671, doi:10.1364/AO.15.000668, 1976.
Lloyd, J., Grace, J., Miranda, A. C., Meir, P., Wong, S-C., Miranda, H. S., Wright, I. R., Gash, J. H. C., and MacIntyre, J. A.: A simple calibrated model of Amazon rainforest productivity based of leaf biochemical properties, Plant Cell Environ., 18, 1129–1145, 1995.
Lloyd, J., Bird, M. I., Veenendaal, E. M., and Kruijt, B.: Should phosphorus availability be constraining moist tropical forest responses to increasing CO_2 concentrations? in: Global Biogeochemical Cycles in the Climate System, edited by: Schulze, E., Heimann, M., Harrison, S., Holland, E., Lloyd, J., Prentice, I. C., Schimel, D., Academic Press, San Diego, CA, 95–114, 2001.
Lovelock, C. E., Kyllo, D., Popp, M., Isopp, H., Virgo, A., and Winter, K.: Symbiotic vesicular-arbuscular mycorrhizae influence maximum rates of photosynthesis in tropical tree seedlings grown under elevated CO_2, Austral. J. Plant Physiol., 24, 185–194, 1997.
Lowman, M. D. and Box, J. D.: Variation in leaf toughness and phenolic content among five species of Australian rain forest trees, Aust. J. Ecol., 8, 17–25, 1983.
Malavolta, E., Vitti, G. C., and de Oliveira, S. A.: Avaliação do estado nutricional das plantas: principios e aplicações. Associação Brasileira para Pesquisa da Potassa e do Fosfato, 1989.
Meir, P., Kruijt, B., Broadmeadow, M., Barbosa, E., Kull, O., Carswell, F., Nobre, A., and Jarvis, P. G.: Acclimation of photosynthetic capacity to irradiance in tree canopies in relation to leaf nitrogen and leaf mass per unit area, Plant Cell Environ., 25, 343–357, 2002.
Mercado, L., Lloyd, J., Dolman, A. J., Stich, S., and Patiño, S.: Modelling basin-wide variations in Amazon forest productivity I. Model calibration, evaluation and upscaling functions for canopy photosynthesis, Biogeosci. Discuss., accepted, 2009.
Monsi, M. and Saeki, T.: Über den Lichtfaktorin den Pflanzengesellschaften und seine Bedeutung für den Stoffproduction, Jap. J. Bot., 14, 14–52, 1953.
Niinemets, U. L.: Photosynthesis and resource distribution through plant canopies. Plant Cell Environ., 30, 1052–1071, 2007.
Olsen, S. R. and Sommers, E. L.: Phosporus Soluble in Sodium Bicarbonate, Methods of Soil Analysis, Part 2, Chemical and Microbiological Properties, edited by: Page, A. L., Miller, P. H., and Keeney D. R., 404–430, 1982.
Ometto, J. P. H. B., Ehleringer, J. R., Domingues, T. F., Ishida, F. Y., Berry, J., Higuchi, N., Flanagan, L., Nardoto, G. B., and Martinelli, L. A..: The stable carbon and nitrogen isotopic

composition of vegetation of the Amazon region, Brazil, Biogeochem. 79, 251–274, 2006.
Parker, G. and Maynard Smith, J.: Optimization theory in evolutionary biology, Nature, 348, 27–33, 1990.
Patiño, S., Lloyd, J., Paiva, R., Baker, T. R., Quesada, C. A., Mercado, L. M., Schmerler, J., Schwarz, M., Santos, A. J. B., Aguilar, A., Czimczik, C. I., Gallo, J., Horna, V., Hoyos, E. J., Jimenez, E. M., Palomino, W., Peacock, J., Peña-Cruz, A., Sarmiento, C., Sota, A., Turriago, J. D., Villanueva, B., Vitzthum, P., Alvarez, E., Arroyo, L., Baraloto, C., Bonal, D., Chave, J., Costa, A. C. L., Herrera, R., Higuchi, N., Killeen, T., Leal, E., Luizão, F., Meir, P., Monteagudo, A., Neil, D., Núñez-Vargas, P., Peuela, M. C., Pitman, N., Priante Filho, N., Prieto, A., Panfil, S. N., Rudas, A., Salomo, R., Silva, N., Silveira, M., Soares deAlmeida, S., Torres-Lezama, A., Vásquez-Martnez, R., Vieira, I., Malhi, Y., and Phillips, O. L.: Branch xylem density variations across the Amazon Basin, Biogeosciences, 6, 545–568, 2009, http://www.biogeosciences.net/6/545/2009/.
Poorter, L., Kwant, R., Hernandez, R., Medina, E., and Werger, M. J. A.: Leaf optical properties in Venezuelan cloud forest trees, Tree Physiol., 20, 519–526, 2000.
Poorter, L., Bongers, L., and Bongers, F.: Architecture of 54 moist-forest tree species: traits, trade-offs, and functional groups, Ecology, 87, 1289–1301, 2006.
Popma, J., Bongers, F., and Werger, M. J. A.: Gap-depdendence and leaf characteristics of trees in a tropical rain forest in Mexico, Oikos, 63, 207–214, 1992.
Portis, A. R.: Regulation of ribulose-1,5-bisphosphate carboxylase/oxygenase activity, Ann. Rev. Plant Physiol. Mol. Biol., 43, 415–437, 1992.
Pottosin, I. I. and Schönkmecht, G.: Ion channel permeable for divalent and monovalent cations in native spinach thylakoid membranes, J. Membr. Biol. 152, 223–233, 1996.
Quesada, C. A., Lloyd, J., Schwarz, M., Czimczik, C., Herrera, R., and Hodnett, M.: Chemical and physical properties of Amazonian forest soils in relation to their genesis, Biogeosci. Discuss., accepted, 2009.
Raaimakers, D., Boot, R. G. A., Dijkstra, P., Pot, S, and Pons, T.: Photosynthetic rates in relation to leaf phosphorus content in pionerr versus climax tropical spewcies, Oecologia, 102, 120–125, 1995.
Raaimakers, D., Boot, R. G. A., Dijkstra, R., Pot, S., and Pons, T.: Photosynthetic rates in relation to leaf phosphorus content in pioneer climax tropical rainforest trees, Oecologia, 102, 120–125, 1995.
Rabash, J., Steele, F., Browne, W., and Prosser, B.: A User's Guide to MLWiN Version 2.0,

Centre for Multilevel Modelling, Institute of Education, University of London, London, UK, 2004.
Reich, P., Ellsworth, D. S., and Uhl, C.: Leaf carbon and nutrient assimilation and concervation in species of differing successional status in an oligotrophic Amazonian forest, Funct. Ecol., 9, 65–76, 1995.
Reich, P. B., Walters, M. B., Ellsworth, D. S., Vose, J. M., Volin, J. C., Gresham, C., and Bowman, W. D.: Relationships of leaf dark respiration to leaf nitrogen, specific leaf area and leaf life-span: a test across biomes and functional groups, Oecologia, 114, 471–482, 1998.
Rijkers, T., Pons, T. L., and Bongers, F.: The effect of tree height and light availability on photosynthetic leaf traits of four neotropical species differing in shade tolerance, Funct. Ecol., 14, 77–86, 2000.
Rozendaal, D. M. A., Hurdato, V. H. and Poorter, L.: Plasticity in leaf traits of 38 tropical tree species in response to light: relationships with light demand and adult stature, Func. Ecol., 20, 207–216, 2006.
Sands, P. J.: Modelling canopy production. II. From single-leaf photosynthetic parameters to daily canopy photosynthesis, Aust. J. Plant Physiol., 22, 603–614, 1995.
Santiago, L. S., Goldstein, G., Meinzer, F. C., Fisher, J. B., Machado, K., Woodruff, D., and Jones, T.: Leaf photosynthetic traits scale with hydraulic conductivity and wood density in Panamanian forest canopy trees, Oecologia, 140, 543–550, 2004.
Sellers, P. J., Collatz, G. J., Randall, D. A., Dazlich, D. A. Zhang, C., Berry, J. A. Field, C. B., Collelo, G. D., and Bounoua, L.: A Revised Land Surface Parameterization (SiB2) for Atmospheric GCMS, Part I: Model Formulation, J. Clim., 9, 676–705, 1996.
Shaul, O.: Magnesium function and transport in plants; the tip of the iceberg, BioMetals, 15, 309–323, 2002.
Sitch, S., Smith, B., Prentice, I. C., Arneth, A. and Bondeau, A.: Evaluation of ecosystem dynamics, plant geography and terrestrial carbon cycling in the LPJ dynamic global vegetation model, Global Change Biol., 9, 161–185, 2003.
Snijders, T. A. B. and Bosker, R. J.: Multilevel analysis, Sage Publications, London, UK, 1999.
Sterck, F. J., Rijkers, T. and Bongers, F.: Effects of tree height and light availability on plant traits at different organisation levels, Monographiae Biologicae, 289–300, 2001.
Stockhoff, B. A.: Maximization of daily canopy photosynthesis: effects of herbivory on optimal nitrogen distribution, J. Theor. Biol., 169, 209–220, 1994.
Sutton, S. L.: The spatial distribution of flying insects, in Tropical Rain Forest Ecosystems.

Bigeographical and Ecological Studies, edited by: Lieth, H., and Werger, M. J. A., Elsevier, Amsterdam, 427–436, 1989.
Terashima, I., Araya, T., Miyazawa, S. I., Sone, K., and Yano, S.: Construction and maintenance of the optimal photosynthetic systems of the leaf, herbaceous plant and tree: an eco-developmental treatise, Ann. Bot.-London, 95, 507, 2005.
Thomas, S. C. and Bazzaz, F. A.: Asymptotic tree height as a predictor of photosynthetic characteristics in Malaysian rain forest trees, Ecology, 80, 1607–1622, 1999.
Thompson, I. J. and Barnett, A. R.: Coulomb and Bessel functions of complex arguments and order, J. Computational Physics, 490–509, 1986.
Turgeon, R.: Phloem loading: how leaves gain their independence, BioScience, 56, 15–24, 2006.
Turner, I. M.: The Ecology of Trees in the Tropical Forest, Cambridge University Press, Cambridge, UK, 2001.
Vitousek, P. M.: Litterfall, nutrient cycling and nutrient limitation in tropical forest, Ecology, 65, 285–298, 1984.
Warren, C. R., Adams, M. A., and Chen, Z. L.: Is photosynthesis related to concentrations of nitrogen and Rubisco in leaves of Australian native plants? Aust. J. Plant Physiol., 27, 407–416. 2000.
Werner, R. A. and Brand, W. A.: Referencing strategies and techniques in stable isotope ratio analysis, Rapid Comm. Mass Spectrom., 15, 501–519, 2001
Werner, R. A., Bruch, B. A., and Brand, W. A.: ConFlo III – An interface for high precision d13C and d15N analysis with an extended dynamic range, Rapid Comm. Mass Spectrom., 13, 1237–1241, 1999.
Wirth, R., Weber, B., and Ryel, R. J.: Spatial and temporal variability of canopy structure in a tropical moist forest, Acta Oecologica, 22, 235–244, 2001.
Woodward, F. I. and Lomas, M. R.: Vegetation dynamics – simulating responses to climatic change, Biol. Rev., 79, 643–670, doi:10.1017/S1464793103006419, 2004.
Wright, I. J., Reich, P. B., Westoby, M., Ackerly, D. D., Baruch, Z., Bongers, F., Cavender-Bares, J., Chapin, T., Cornelissen, J. H., Diemer, M., Flexas, J., Garnier, E., Groom, P. K., Gulias, J., Hikosaka, K., Lamont, B. B., Lee, T., Lee, W., Lusk, C., Midgley, J. J., Navas, M. L., Niinemets, U., Oleksyn, J., Osada, N., Poorter, H., Poot, P., Prior, L., Pyankov, V. I., Roumet, C., Thomas, S. C., Tjoelker, M. G., Veneklaas, E. J., and Villar, R.: The worldwide leaf economics spectrum, Nature, 428, 821–827, 2004.

Wright, I. J. Leishman, M. R., Read, C., and Westoby, M: Gradients of light availability and leaf traits with leaf age and canopy position in 28 Australian shrubs and trees, Func. Plant Biol., 43, 407–419, 2006.

Table 1. Different potential "optimal" values of leaf area index, L, and associated decay coefficients for photosynthetic capacity through the canopy, k_P (in brackets) for various combinations of total canopy photosynthetic capacity, C_C expressed in μmol m^{-2} (ground area) s^{-1}, and photosynthetic capacity for leaves art the top of the canopy in the absence of dark respiration , A_0^*, expressed in μmol m^{-2} (leaf area) s^{-1}. Three values are given (in order); that where the photosynthetic productivity is maximised as in Fig. 4 (i.e. with no consideration of "evolutionarily stable" strategies or the need for the light compensation point, for the lowest leaves to be greater than zero; denoted "a"; that where the "evolutionarily stable" L has been estimated as in Eq. 4, denoted "b"; that where the long term light compensation point is equal to zero (i.e. photosynthesis exactly balanced respiration for the lowest leaves of the canopy over a 3.5 year period; denoted "c". NR="Notreached" which means this point occurred above the maximum tested leaf area index of 10.0; ND="Notdetermined", usually because the value of k_P required to fulfil these simulations was <0.0 (see text). Values in bold suggest the most likely values (see text) and lightly shaded cells correspond to the "optimal" solutions as shown in Fig. 4.

	Model	C_C=15.75	C_C=21.0	C_C=31.5	C_C=42.0	C_C=52.5	C_C=63.0
A_0^*=6	a	5.1(0.29)	4.3 (0.10)	ND	ND	ND	ND
	b	NR	**7.2 (0.23)**	ND	ND	ND	ND
	c	NR	7.4 (0.24)	ND	ND	ND	ND
A_0^*=12	a	NR	8.9 (0.57)	5.4 (0.31)	4.6 (0.12)	4.2 (0.00)	ND
	b	NR	NR	8.4 (0.36)	6.7 (0.22)	5.9 (0.10)	ND
	c	NR	NR	**7.9 (0.36)**	**5.5 (0.18)**	**4.5 (0.01)**	ND
A_0^*=18	a	NR	NR	9.4 (0.57)	6.2 (0.39)	5.1 (0.24)	4.7 (0.14)
	b	NR	NR	NR	9.0 (0.42)	7.4 (0.30)	6.6 (0.22)
	c	NR	NR	NR	**8.0 (0.41)**	**5.5 (0.26)**	**4.5 (0.12)**

BGD
6, 4639–4692, 2009

Table 2. Estimated intercept and coefficients according to Eq. (13) for leaf mass per unit area, leaf [N], leaf [C] , leaf δ^{13}C, leaf [P], leaf [Ca], leaf [Mg] and leaf [K] all expressed on a leaf dry weight basis.

	Log_e [Leaf mass/area] (g m^{-2})		Log_e [Nitrogen] (mg g^{-1})		$\text{Log}_e\lvert\delta^{13}\text{C}\rvert$ (‰)		Log_e [Carbon] (mg g^{-1})	
Fixed effect	Coefficient	S.E.	Coefficient	S.E.	Coefficient	S.E.	Coefficient	S.E.
γ_{000}= Intercept	4.560	0.0270	3.004	0.0267	3.673	0.0032	6.185	0.0077
γ_{100}= Coefficient of h	**0.00981**	**0.00123**	−0.00121	0.00081	**–0.00151**	**0.00019**	**0.00114**	**0.00018**
γ_{010}= Coefficient of ($h_C - h$)	0.00104	0.00354	0.00332	0.00329	0.00013	0.00048	0.00036	0.00082
Random Effect	Parameter	S.E.	Parameter	S.E.	Parameter	S.E.	Parameter	S.E.
φ_0^2=between plot variance	0.01693	0.00689	0.01783	0.00689	0.00026	0.00009	0.00201	0.00058
τ_0^2=between tree variance	0.06047	0.00757	0.05876	0.00711	0.00747	0.00010	0.00334	0.00041
σ_0^2=within tree variance	0.01382	0.00099	0.00611	0.00044	0.00033	0.00002	0.00028	0.00003
	Log_e [Phosphorus] (mg g^{-1})		Log_e [Calcium] (mg g^{-1})		Log_e [Magnesium] (mg g^{-1})		Log_e [Potassium] (mg g^{-1})	
Fixed effect	Coefficient	S.E.	Coefficient	S.E.	Coefficient	S.E	Coefficient	S.E.
γ_{000}=Intercept	−0.1244	0.0508	1.532	0.098	0.6991	0.0485	1.646	0.070
γ_{100}=Coefficient of h	−0.00107	0.00130	−0.00520	0.00320	**–0.00684**	**0.00218**	**–0.00538**	**0.00220**
γ_{010}=Coefficient of ($h_C - h$)	0.00206	0.00460	0.00106	0.00937	**0.01490**	**0.00642**	−0.00853	0.00604
Random Effect	Parameter	S.E.	Parameter	S.E.	Parameter	S.E.	Parameter	S.E.
φ_0^2=between plot variance	0.10919	0.02691	0.41396	0.09744	0.05785	0.02232	0.22444	0.04989
τ_0^2=between tree variance	0.09322	0.01150	0.30900	0.04009	0.18150	0.02292	0.12120	0.01604
σ_0^2=within tree variance	0.01519	0.00109	0.09229	0.00663	0.04282	0.00307	0.04371	0.00314

BGD
6, 4639–4692, 2009

Table 3. Estimated intercept and coefficients according to Eq. (13) for leaf [N], leaf [C] , leaf [P], leaf [Ca], leaf [Mg] and leaf [K], all expressed on a leaf area basis.

	Log_e [Nitrogen] (mg m^{-2})		Log_e [Carbon] (mg m^{-2})		Log_e [Phosphorus] (mg m^{-2})	
Fixed effects	Coefficient	S.E.	Coefficient	S.E.	Coefficient	S.E.
γ_{000}=Intercept	7.572	0.021	10.75	0.011	4.448	0.0475
γ_{100}=Coefficient of h	**0.00873**	**0.00136**	**–0.01112**	**0.00135**	**0.00893**	**0.00167**
γ_{010}=Coefficient of $(h_C - h)$	0.00372	0.00351	0.00066	0.00426	0.00465	0.00398
Random Effects	Parameter	S.E.	Parameter	S.E.	Parameter	S.E.
φ_0^2=between plot variance	0.00215	0.00463	0.02856	0.01155	0.09834	0.02210
τ_0^2=between tree variance	0.05775	0.00773	0.06670	0.00850	0.05822	0.00782
σ_0^2=within tree variance	0.01642	0.00135	0.01521	0.00119	0.02460	0.00226
	Log_e [Calcium] (mg m^{-2})		Log_e [Magnesium] (mg m^{-2})		Log_e [Potassium] (mg m^{-2})	
Fixed effects	Coefficient	S.E.	Coefficient	S.E.	Coefficient	S.E
γ_{000}=Intercept	6.126	0.0979	5.268	0.0498	6.232	0.07187
γ_{100}=Coefficient of h	0.00372	0.00234	0.00264	0.00244	**0.004425**	**0.00223**
γ_{010}=Coefficient of $(h_C - h)$	−0.00156	0.00654	**0.01712**	**0.00700**	−0.00155	0.00654
Random Effects	Parameter	S.E.	Parameter	S.E.	Parameter	S.E.
φ_0^2=between plot variance	0.3553	0.0915	0.05574	0.02276	0.3553	0.09146
τ_0^2=between tree variance	0.3867	0.0538	0.18610	0.02458	0.3867	0.05381
σ_0^2=within tree variance	0.1072	0.0072	0.05135	0.00388	0.1072	0.00721

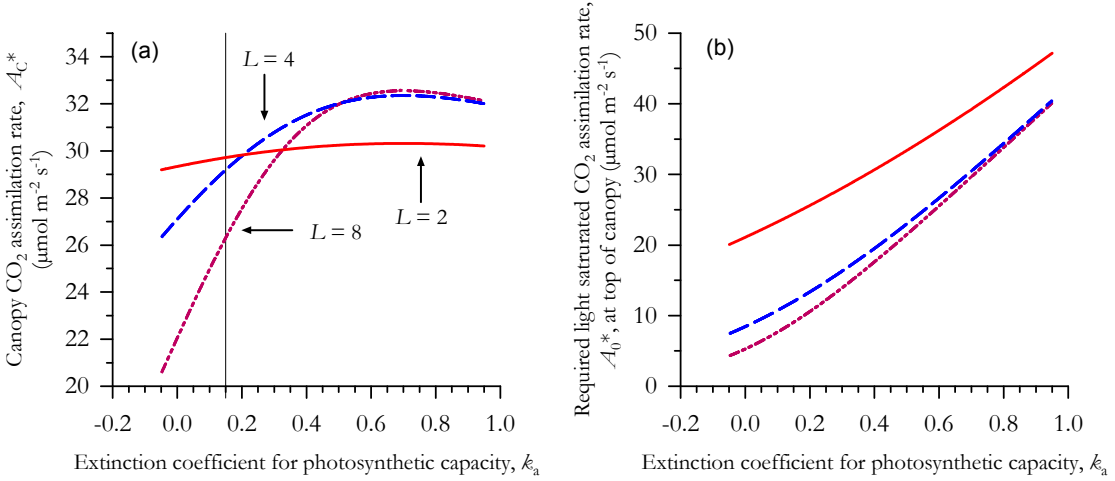

Fig. 1. Effect of variations in extinction coefficient for photosynthetic capacity at a range of different leaf area indices, L. **(a)** variations in canopy CO_2 assimilation rate; **(b)** required photosynthetic assimilation rate at the top of the canopy.

BGD
6, 4639–4692, 2009

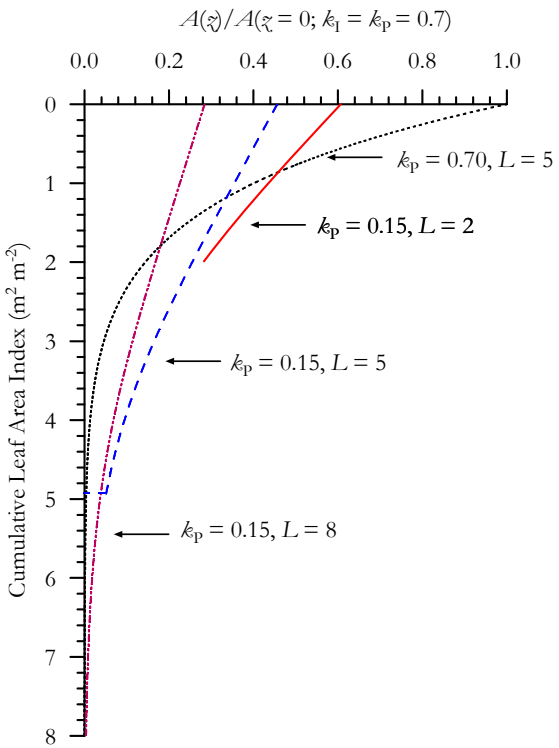

Fig. 2. Variations in the rate of photosynthesis (A) with canopy depth (z), normalised to that which would occur at the top of the canopy when the extinction coefficient for photosynthetic capacity, k_P, is equal to that for light, k_I which has in this case been set at 0.7. Values are shown for different combinations of k_P and leaf area index , L.

BGD
6, 4639–4692, 2009

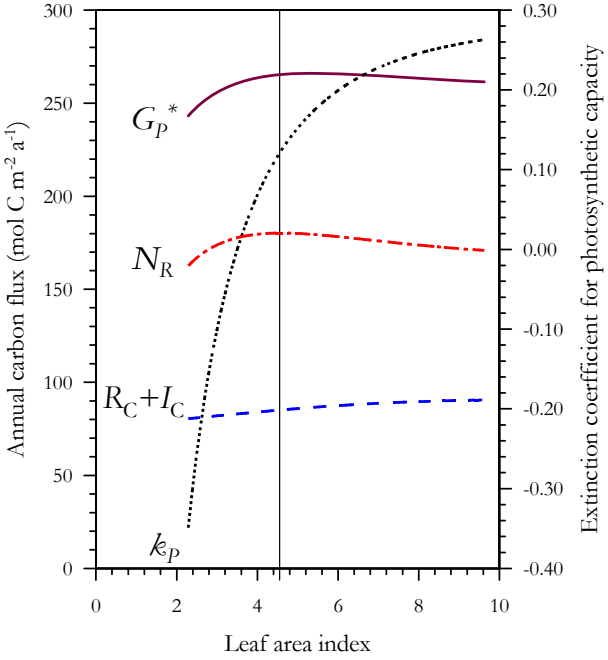

Fig. 3. Variations in the rate of Gross Primary production (in the absence of any leaf respiration in the light), G_P^*, the sum of leaf respiration (day and night) plus investment costs in leaf construction (R_C+I_C) and the difference between the two, the annual net carbon gain of the canopy, N_R as defined through Eq. (2) as a function of leaf area index. Associated variations in the extinction coefficient for photosynthetic capacity, k_P, are also shown.

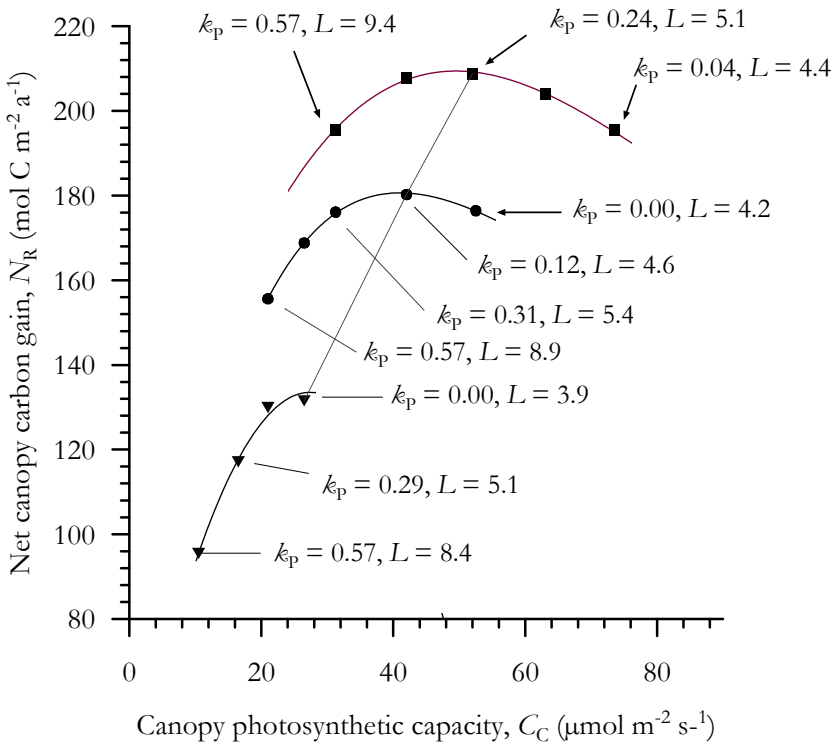

Fig. 4. Relationship between net canopy carbon gain (as defined by Eq. 2) and canopy photosynthetic capacity according to the model presented in Appendix A. Curves shown are for different photosynthetic capacities, A_0, at the top of the canopy; ▼: A_0=6 μmol m^{-2} s^{-1}; ●: A_0=12 μmol m^{-2} s^{-1}; ■: A_0=18 μmol m^{-2} s^{-1}.

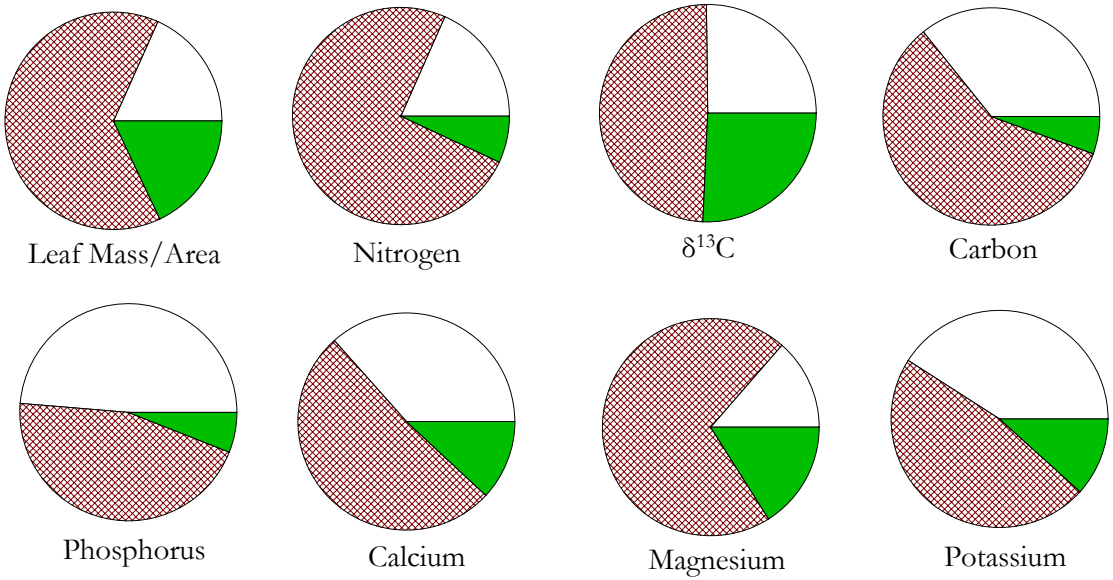

Fig. 5. Partitioning of the observed variance in the dataset according to Eq. (14). Green=variability with height within individual trees; purple hatches; variability between trees within individual plots; white=variability between plots.

BGD
6, 4639–4692, 2009

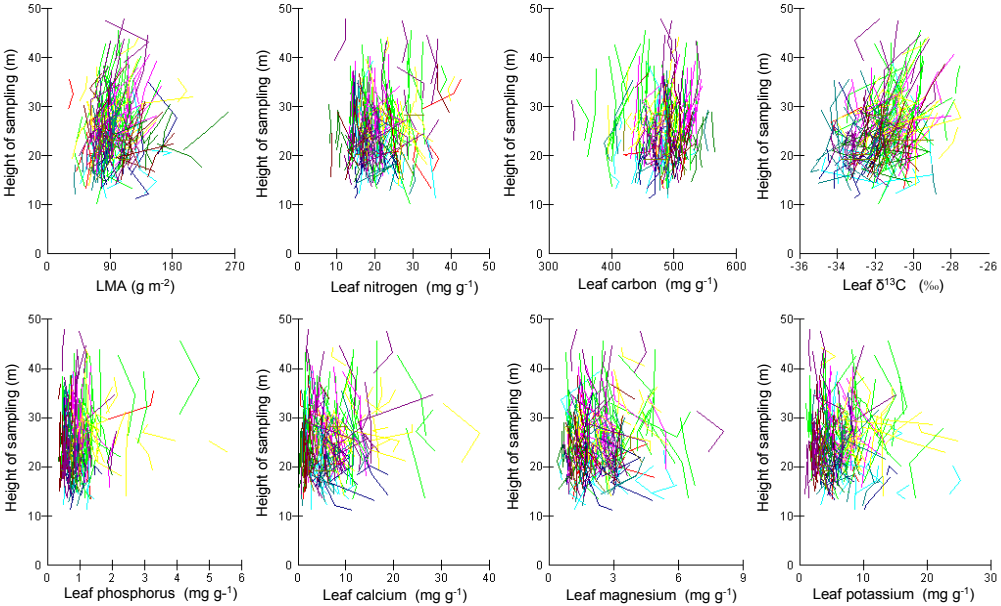

Fig. 6. Vertical gradients in leaf mass per unit area, leaf [N], leaf [C] , leaf δ^{13}C, leaf [P], leaf [Ca], leaf [Mg] and leaf [K] for 204 trees sampled across Amazonia. Different colours refer to different regions out outlined in the Supplementary information.

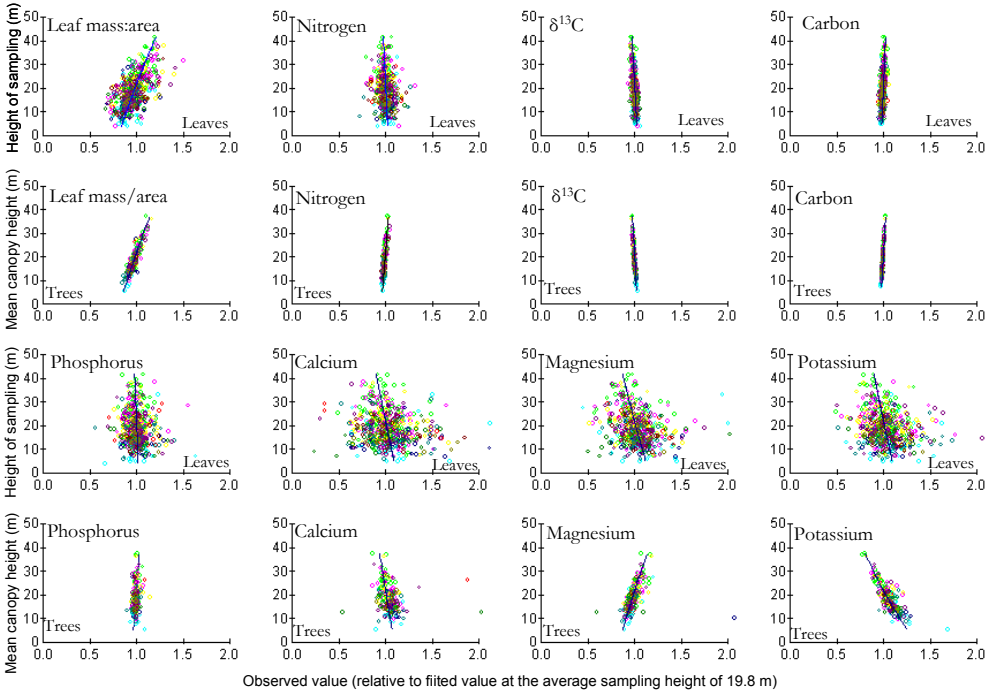

Fig. 7. Observed values and fitted lines for within tree gradients ("Leaves") and tree-to-tree gradients ("Trees") for leaf mass per unit area, leaf [N], leaf [C] , leaf δ^{13}C, leaf [P], leaf [Ca], leaf [Mg] and leaf [K] for 204 trees sampled across Amazonia. Different colours refer to different regions out outlined in the Supplementary information.

BGD
6, 4639–4692, 2009

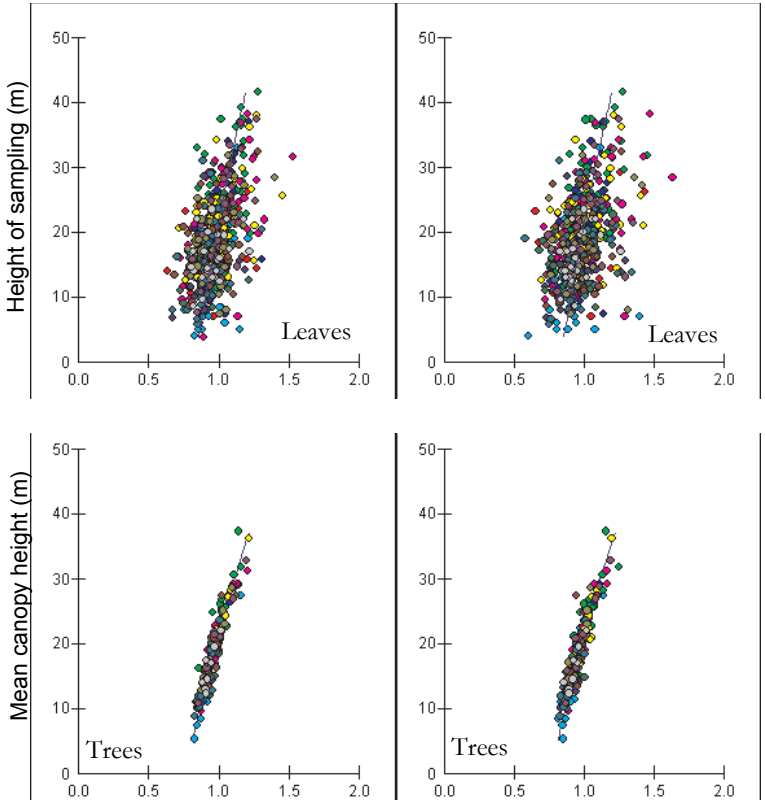

Fig. 8. Vertical gradients in leaf [N], and leaf [P] expressed on a leaf area basis. Different colours refer to different regions out outlined in the Supplementary information.

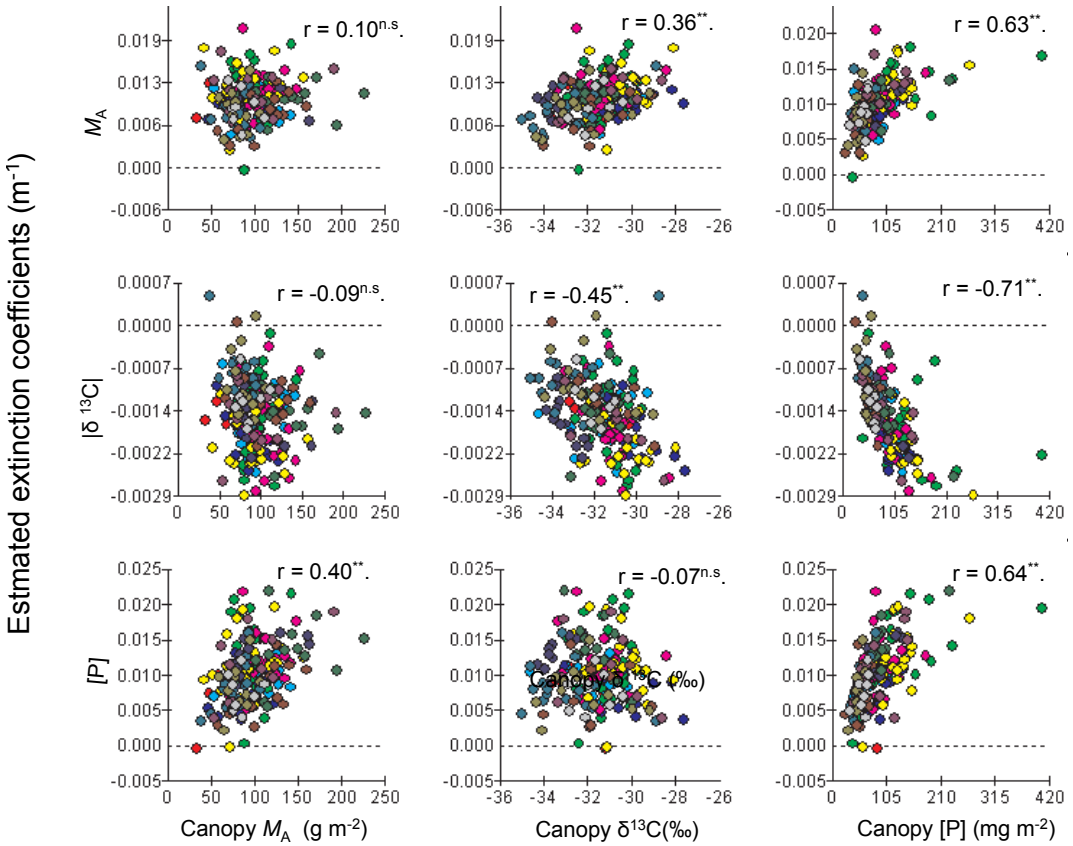

Fig. 9. Relationship between within canopy gradients in leaf mass per unit area (M_A), foliar $\delta^{13}C$ and leaf phosphorus concentrations (area basis) and the overall mean M_A $\delta^{13}C$ and [P] in the same tree. Also shown are Spearman's rank correlation coefficients and their level of significance (*; 0.P<0.05; **; P<0.01).

BGD
6, 4639–4692, 2009

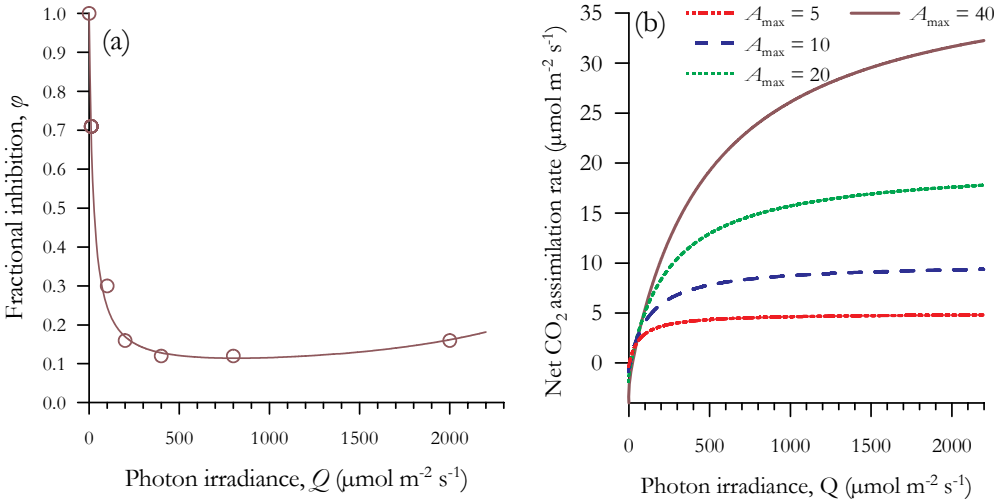

Fig. A1. Key features of the model. **(a)** Inhibition of leaf respiration in the light (Eq. A6); **(b)** Predicted variations net CO_2 assimilation rates for a range of A_{max} including the allowance for of inhibition of leaf respiration in the light (Eq. A1).

BGD
6, 4639–4692, 2009